U.PORTO

MESTRADO
MEDICINA E ONCOLOGIA MOLECULAR

Deciphering Epitranscriptomic Signature: the Role of 5-Methylcytosine in Prostate Cancer

Patrícia Ferreira da Torre

M

2024

Patrícia Ferreira da Torre

Deciphering Epitranscriptomic Signature: the Role of 5-Methylcytosine in Prostate Cancer

Dissertação de Candidatura ao grau de **Mestre em Medicina e Oncologia Molecular** submetida à Faculdade de Medicina da Universidade do Porto

Orientadora: **Professora Doutora Carmen de Lurdes Fonseca Jerónimo**
Professora Catedrática Convidada
Departamento de Patologia e Imunologia Molecular
Instituto de Ciências Biomédicas Abel Salazar, Universidade do Porto
Diretora do Centro de Investigação, Coordenadora e Investigadora Auxiliar
Grupo de Epigenética & Biologia do Cancro – Centro de Investigação
Instituto Português de Oncologia do Porto Francisco Gentil E.P.E.

Coorientadora: **Doutora Vera Mónica Miranda Gonçalves**
Investigadora Júnior
Grupo de Epigenética & Biologia do Cancro – Centro de Investigação
Instituto Português de Oncologia do Porto Francisco Gentil E.P.E.

"For me, I am driven by two main philosophies: know more today about the world than I knew yesterday and lessen the suffering of others. You'd be surprised how far that gets you."

Neil deGrasse Tyson

This project was funded by a grant from the Research Centre of Portuguese Oncology Institute of Porto: DECODE PCa (PI 157–CIPOP–121–2019)

AGRADECIMENTOS

Quando na licenciatura iniciei o meu percurso no Grupo de Biologia e Epigenética do Cancro, há mais de dois anos, estava longe de imaginar toda a evolução que viria a ter, quer como investigadora, quer como pessoa. Por isto, devo o meu obrigada a diversas pessoas que tornaram o meu desenvolvimento possível:

À Professora Doutora Carmen Jerónimo, na qualidade de diretora do Centro de Investigação do IPO Porto, coordenadora do grupo e minha orientadora, por me ter recebido de braços abertos, tanto na licenciatura como no mestrado, e por demonstrar toda a disponibilidade para ajudar a superar os desafios que foram surgindo. Obrigada por ter acreditado sempre nas minhas capacidades!

À Vera, a minha coorientadora, por estar sempre disponível para me ajudar em todos os percalços que foram surgindo ao longo do projeto. Quer seja nas células, nos microscópios, e acima de tudo nos Western Blots, obrigada por me mostrares que há sempre uma solução e uma aprendizagem a retirar. Foste sem dúvida uma peça extremamente essencial para o meu mestrado!

À Catarina Teixeira, carinhosamente a minha Teixas e minha parceira da Epitranscriptómica, que também funcionou como orientadora "off record", por todos os momentos de aprendizagem (sejam eles de ciência ou não), de gargalhadas e muita felicidade, que foram cruciais para manter o equilíbrio ao longo destes dois anos. Sem o teu apoio nada teria sido possível! O meu muito obrigada, és especial!

O meu mais profundo obrigada à Diana, Marmita, Mariana, Nanda, Ângela e à Diana Fonseca, as minhas meninas da sala de mestrado, por terem sido a melhor fonte de conversas e risos à hora do almoço, e a melhor forma de apoio dentro do laboratório para todos os momentos desafiantes que existiram neste projeto. Na categoria de adoração, vocês seriam todas um 10.

A todos os restantes membros atuais ou passados do grupo, especialmente à Dani, que foi a catalisadora da minha dissertação e a pessoa responsável pelos primeiros passos que dei no laboratório, o meu muito obrigada, nada disto teria sido possível sem vocês, juntos fazemos uma equipa imbatível!

Aos meus pais, sem dúvida os meus maiores apoiantes deste o primeiro dia. Mãe, obrigada por seres o meu maior modelo de vida, e por toda a dedicação que pões na nossa família. Pai, obrigada por mostrares todo o carinho, amor e orgulho deste mundo na menina dos teus olhos. Esta dissertação é especialmente para vocês, amo-vos imenso.

À minha restante família, especialmente ao meu irmão, aos meus avós e às minhas tias Linda e Glória. Não acredito na minha tamanha sorte na família que tenho, por todo o apoio que sempre me deram, o meu obrigada.

Ao Leo, que esteve comigo desde o primeiro até ao último ano da universidade, e que foi o melhor colega de casa e amigo que podia pedir. Obrigada por todas as vezes que me alegraste sempre que chegava a casa cansada e desanimada, por todas as viagens do pingo doce a casa carregados, e por todos os pânicos coletivos a matar aranhas em casa, partilharemos sempre o mesmo neurónio!

À Sara, a minha confidente e única pessoa capaz de me pôr um sorriso na cara independentemente da situação. Nestes anos, conseguiste tornar-te tanto para mim, e só estou imensamente grata por tudo, desde os jantares em minha casa, idas ao jardim para tocar em relva, aulas de mindfullness no ginásio, referências extremamente niche que me fazem rir até colapsar, e muita mais coisa que não vou escrever aqui, mas que só nós sabemos. Ser tua amiga tem sido um prazer enorme e uma descoberta diária maravilhosa, obrigada por todos os momentos e palavras, contigo a vida é efetivamente um morango!

A todos os meus restantes amigos, a Rita, a Catarina, o Rodrigo, a Lipa, os PoPos, a Raquel, a Cláudia, o Tommy, o Edu, o Jorginho, os meus FMUPers e todas as pessoas que preencheram de bons momentos estes últimos cinco anos, sou-vos muito grata por tudo.

Um obrigada também aos professores que passaram pelo meu percurso, da FCUP, FMUP e ICBAS, foram absolutamente essenciais para a minha formação universitária, e permitiram-me descobrir o que verdadeiramente gosto de fazer, o meu muito obrigada!

Por fim, mas não menos importante, quero agradecer à pessoa que me despertou o interesse neste mundo tão complexo e fascinante que é a Oncologia, a minha tia Maria José. Tal como na licenciatura, repito as minhas palavras, que nunca irão parar de ser as mesmas: o meu percurso ainda é recente, mas garanto que muito mais estará para vir. Apesar de já não te poder dizer pessoalmente, obrigada por me teres dotado de imensa resiliência e bondade, darei sempre o meu melhor para tornar outras vidas melhores.

"Aqueles que passam por nós, não vão sós, não nos deixam sós. Deixam um pouco de si, levam um pouco de nós." Obrigada a todos que deixaram um pouco deles e levaram um pouco de mim!

RESUMO

Introdução: O cancro da próstata (CaP) é o segundo tumor mais incidente e a quinta causa de morte relacionada com o cancro em todo o mundo. A sua natureza heterogénea representa um obstáculo importante no tratamento e gestão clínica dos doentes. Assim, descobrir novas assinaturas moleculares permanece uma necessidade urgente, de forma a melhorar a estratificação de doentes e otimizar as intervenções terapêuticas.

A 5-metilcitosina (m^5C) é uma das modificações do RNA mais comuns nos mamíferos. As suas proteínas reguladoras, capazes de adicionar, ler ou retirar a marca de metilação, têm sido associadas ao processo carcinogénico, incluindo o CaP. Adicionalmente, esta modificação foi descrita como um potencial biomarcador preditivo para a tomada de decisões de tratamento noutras doenças.

Contudo, a compreensão do papel da marca m^5C no CaP é ainda limitada. Assim, o principal objetivo deste estudo é caraterizar de forma abrangente a marca m^5C e respetivas proteínas reguladoras no CaP.

Métodos: Foi realizada uma análise *in silico* utilizando o The Cancer Genome Atlas (TCGA), onde as proteínas relacionadas com m^5C foram avaliadas no CaP. Os níveis de transcrição dos genes mais desregulados, *YTHDF2*, *NOP2*, *NSUN2* e *NSUN6* foram avaliados numa série de doentes com CaP tratados com prostatectomia radical no IPO Porto. Ensaios imunohistoquímicos (IHQ) para a proteína de NSUN2 foram realizados na mesma série, e os resultados foram analisados de acordo com a informação clinico-patológica, designadamente grau e estadio tumoral.

Os níveis de NSUN2 e NOP2 foram avaliados por transcrito e Western Blot em diferentes linhas celulares de CaP e não-malignas. O gene *NSUN2* foi silenciado com sucesso por transdução com shRNA na linha celular C4-2B. Caracterização de níveis de transcrito e de proteínas associadas à Transição Epitélio-Mesênquima (TEM) foi realizada nas células C4-2B com *NSUN2* shRNA.

Resultados: Vários efetores da marca m^5C, incluindo *NSUN2*, encontram-se significativamente aumentados na série de CaP do TCGA comparativamente com amostras normais. Relativamente aos doentes com CaP do IPO Porto, níveis mais elevados de transcrito de *NSUN2* associaram-se significativamente com tumores menos diferenciados e de estadios mais avançados. Observou-se ainda uma associação significativa entre scores e intensidades de NSUN2 mais elevadas e grupos de graduação mais elevados, bem como estadios mais avançados, em concordância com a análise dos transcritos.

Adicionalmente, as linhas celulares de CaP apresentaram níveis contrastantes de transcrito de *NSUN2* comparativamente às linhas não-malignas, sendo especialmente mais elevados na linha celular C4-2B. A transfeção de shRNA

NSUN2 promoveu com sucesso a diminuição de expressão de NSUN2 nas células C4-2B.

As proteínas relacionadas com a TEM aparentam níveis aumentados na linha celular *NSUN2* knockdown, enquanto parte das proteínas com associação ao fenótipo epitelial demonstram diminuição de valores. Contudo, a NSUN2 não parece ter um papel relevante na regulação da TEM em CaP.

Conclusões: Níveis elevados da proteína NSUN2 encontram-se associados a CaP menos diferenciados, bem como a estadios de tumor mais avançados. Os resultados deste estudo indicam um envolvimento da proteína reguladora NSUN2 em CaP, sugerindo uma função potencialmente oncogénica nesta neoplasia.

Palavras-chave: Cancro da próstata; 5-Metilcitosina; Epitranscriptómica; NSUN2

ABSTRACT

Background: Prostate Cancer (PCa) ranks as the 2nd most incident cancer and 5th most leading cause of cancer-related deaths worldwide. Its heterogeneous nature presents a significant hurdle in treatment and patient management. Thus, there remains a critical need to discover new molecular signatures to improve patient stratification and optimize therapeutic interventions.

5-Methylcytosine (m^5C) is one of the most prevalent RNA modifications in mammals. Its regulatory proteins, capable of adding, reading or removing the methylation mark, have been implicated in cancer, including PCa. Furthermore, this modification was described as a potential predictive biomarker for treatment decision-making in other malignancies.

Nonetheless, understanding of the role of m^5C modification in PCa is still scarce. Hence, the primary aim of this study is to comprehensively characterize m^5C modification and its associated regulatory proteins in PCa.

Methods: An *in silico* analysis was performed using The Cancer Genome Atlas (TCGA), where m^5C-related proteins were evaluated in PCa. The transcript levels of the most deregulated genes, *YTHDF2*, *NOP2*, *NSUN2* and *NSUN6* were assessed in a series of PCa patients treated with radical prostatectomy at IPO Porto. Immunohistochemical (IHC) assays for NSUN2 protein were carried out in the same series, and the results were analyzed according to standard clinicopathological variables, namely tumor grade and stage.

Additionally, NSUN2 and NOP2 transcript and protein levels were evaluated in different PCa and non-malignant cell lines. The *NSUN2* gene was successfully knocked down by shRNA in the C4-2B cell line. Moreover, the characterization of transcript and protein levels associated with Epithelial-Mesenchymal Transition (EMT) was performed in C4-2B cells with *NSUN2* shRNA.

Results: Several m^5C players, including *NSUN2*, were significantly increased in the TCGA PCa series compared to normal samples. Regarding IPO Porto PCa patients, higher *NSUN2* transcript levels were significantly associated with cases of less differentiated tumors and more advanced stages. There was also a significant association between higher NSUN2 IHC scores and intensities and higher group gradings, as well as more advanced stages, in agreement with the transcript analysis.

In addition, PCa cell lines showed contrasting *NSUN2* transcript levels compared to non-malignant lines, being especially higher in the C4-2B cell line. Transfection of *NSUN2* shRNA successfully promoted decreased NSUN2 expression in C4-2B cells. EMT-related proteins showed increased levels in the *NSUN2* knockdown cell line,

while some of the proteins associated with the epithelial phenotype were decreased. However, NSUN2 does not appear to have a relevant role in EMT in PCa.

Conclusions: High levels of NSUN2 protein were associated with less differentiated PCa, as well as more advanced tumor stages. The results of this study indicate an involvement of this protein in PCa, suggesting a potentially oncogenic function in this neoplasm.

Keywords: Prostate cancer; 5-Methylcytosine; Epitranscriptomics; NSUN2

TABLE OF CONTENTS

FIGURES INDEX

TABLES INDEX

LIST OF ABBREVIATIONS

Symbols

Ψ – Pseudouridine

A

ADT – Androgen Deprivation Therapy

ALYREF – Aly/REF Export Factor

AMV – Avian Myeloblastosis Virus

AR – Androgen Receptors

B

BMI – Body Mass Index

BPH – Benign Prostatic Hyperplasia

C

cDNA – Complementary DNA

CP – Cystoprostatectomy

CRPC – Castration-Resistant Prostate Cancer

D

DAB – 3,3'-Diaminobenzidine Tetrahydrocloride Cromogen

DNMT2 – DNA Methyltransferase 2

DRE – Digital Rectal Examination

E

ECL – Enhanced Chemiluminescence

EDTA – Ethylenediamine Tetraacetic Acid

EMT – Epithelial-Mesenchymal Transition

F

FBS – Fetal Bovine Serum

FITC – Fluorescein Isothiocyanate

G

GAPDH – Glyceraldehyde 3-Phosphate Dehydrogenase

GEPIA – Gene Expression Profiling Interactive Analysis

GG – Group Grading

H

HDI – Human Development Index

HG-PIN – High Grade Prostatic Intraepithelial Neoplasia

hm^5C – 5-Hydroxymethylcytosine

I

IHC – Immunohistochemistry

IPO Porto – Portuguese Oncology Institute of Porto

ISUP – International Society of Urological Pathology

L

lncRNA – Long Non-coding RNAs

M

m^1A – N1-Methyladenosine

m^5C – 5-Methylcytosine

m^6A – N6-Methyladenosine

m^7G – N7-Methylguanosine

MET – Mesenchymal-Epithelial Transition

Me-RIP – Methylated RNA Immunoprecipitation

MOI – Multiplicity of Infection

N

ncRNA – Non-coding RNA

Nm – 2'-O-Methylation

NSUN – NOP2/SUN RNA Methyltransferase

P

PBS – Phosphate Buffered Saline

PCa – Prostate Cancer

PCA3 – Prostate Cancer Gene 3

PHI – Prostate Health Index

PIC – Protease Inhibitor Cocktail

PRAD – Prostate Adenocarcinoma

PSA – Prostate Specific Antigen

PSA-D – Prostate Specific Antigen Density

R

RIPA – Radioimmunoprecipitation Assay

RMPs – RNA-Modifying Proteins

RT – Reverse Transcriptase

RT-qPCR – Real-Time quantitative PCR

S

SDS – Sodium Dodecyl Sulphate

SDS-PAGE – Sodium Dodecyl Sulphate-Polyacrylamide Gel Electrophoresis

T

TCGA – The Cancer Genome Atlas

TET – Ten-Eleven Translocation

TGF-β – Transforming Growth Factor Beta

TRDMT1 – tRNA Aspartic Acid Methyltransferase 1

TurboGFP – Turbo Green Fluorescent Protein

Y

YBX1 – Y-box Binding Protein 1

YTHDF2 – YTH Domain-containing Family 2

INTRODUCTION

Cancer: a global health management challenge

Cancer has been considered a major concern worldwide: besides being an important barrier against the global increase in life expectancy, it presents itself as a major economic and societal burden [1]. It is estimated that between 2020 and 2050, the global economic cost of cancer will be 25.2 trillion US dollars [2]. Besides this, socioeconomic imbalances that may affect treatment can cause distress for the patient [3].

According to GLOBOCAN, in 2022, cancer is responsible for one in six deaths in the world. In terms of premature deaths, three in ten are caused by this disease. As the numbers increase progressively within the decades, the future predictions reveal themselves as an even bigger challenge: by 2050, it is projected that 35 million new cases will emerge, meaning a 77% increase from 2022 [1]. This is a direct result of the populational growth, especially in low and medium Human Development Index (HDI) countries [1].

Prostate cancer

Disease insights: incidence, mortality and risk factors

Based on World Health Organization (WHO), prostate cancer (PCa) is the second most incident and the fifth cause of cancer-related death in males in the world. In almost two thirds of the world's countries (118 of 185), PCa is the most frequently diagnosed cancer among men (***Figure 1***), along with the leading cause of cancer death among men in 52 countries. As of 2022, an estimated 1.5 million new cases were diagnosed, and almost 400,000 deaths occurred due to PCa [1].

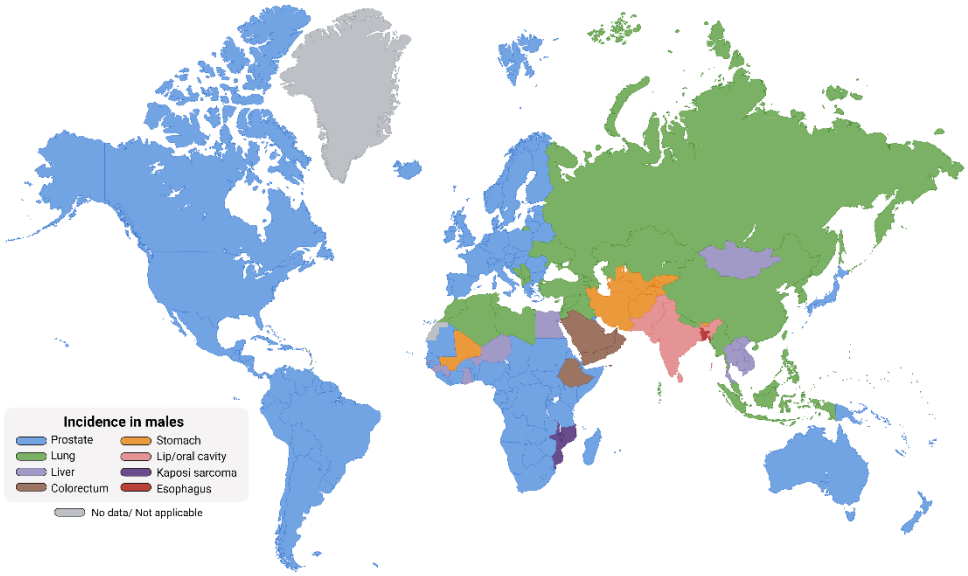

***Figure 1*. World map of the most incident cancer in males in each country, as of 2022.** PCa is the most common cancer in several countries. Information taken from [1]. Created with BioRender.com

Furthermore, PCa is particularly incident in transitioned countries with a high or very high HDI (35.5 per 100,000 males, versus 12.6 in low HDI countries), mainly due to eased access to targeted population screening and diagnostic practices [1, 4]. Contrastingly, the mortality rates are very similar between high HDI and low HDI countries (7.3 and 6.6 deaths per 100,000 males, respectively) [1].

PCa is believed to first originate from a precursor lesion known as high grade prostatic intraepithelial neoplasia (HG-PIN), thus being suggested as a transition phase. HG-PIN presents abnormal cytological features in the glands or ducts of epithelial cells in the prostate [5]. PCa is commonly divided by three subtypes, in order of risk: clinically localized PCa, which is treatment naïve; metastatic PCa, still sensitive to hormones; and castration-resistant PCa (CRPC), metastatic and insensitive to hormones, known as the most lethal type of PCa [5]. Most PCa diagnoses occur in the localized stage (75 to 80%), yet around 35% of patients relapse and metastasize, potentially evolving to CRPC in 10-20% of all cases [5].

The development of PCa is associated with several risk factors (***Figure 2***). Age is the most well-established risk factor, as it is known that men with advanced age are progressively more susceptible to developing [4]. Additionally, having family history of PCa significantly enhances the risk of developing of this disease. Studies have shown that men have more than double the probability of developing PCa when their parent or sibling have been diagnosed [6]. Ethnicity also plays a role in the increased risk: men with African ethnicity, especially from sub-Saharan Africa have higher chances of PCa developing. It is speculated that higher prevalence of certain genetic factors, such as variants of chromosome 8q24 (which contains at least 3 independent risk regions for PCa) [7], *BCL2* (cell apoptosis gene) and *EphB2* (tumor suppression gene) mutations may be related [4, 6].

Moreover, some lifestyle factors are known to increase the risk of PCa. Major factors include obesity/high Body Mass Index (BMI), which has been associated with aggressive PCa and cancer-specific mortality [8]; smoking, as cigarette components have been associated with DNA damage and therefore carcinogenic action, as well as inducing of higher circulating hormone levels like testosterone and androsterone, that contribute to PCa risk and overall cancer progression, and alcohol consumption [6]. Lastly, despite no associated biological mechanisms have been proved, vasectomies have also been linked to an increased risk of PCa development [6].

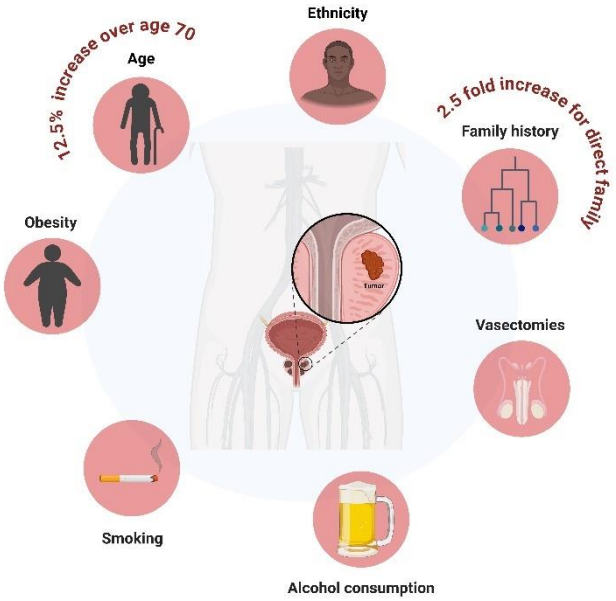

Figure 2. **Risk factors associated with PCa.** Age, ethnicity and family history are the main risk factors among all. Information taken from [4, 6, 7]. Created with BioRender.com.

Classifying Prostate Cancer: Gleason Score and Group Gradings

Since the first medical PCa description, made by Dr. John Adams in 1853 [9], there has been a need to categorize it, as a way to achieve better prognosis, diagnosis and more personalized treatment for each patient. In 1966, Dr. Donald Gleason developed a grading and scoring system for PCa, the Gleason score. This scoring system is based on the histological characteristics of the PCa tissues from each patient and uses a classification scale of the patterns ranging from 1 to 5, where 1 is the most differentiated, and 5 is the least differentiated. The scoring is made by the sum of the first and second most predominant histological patterns, and therefore ranges from 2 to 10 [10].

The Gleason score has since then been the most prevalent scoring system for PCa management worldwide. However, some classification aspects of the scoring have been changed. Pathologists found that scores between 2 and 5 were rarely assigned, and concluded that the classification needed important updates [11]. The International Society of Urological Pathology (ISUP) determined at consensus conferences in 2005, 2014, and most recently in 2019, the introduction of several updates for the Gleason score, named Modified ISUP Gleason score. The Modified ISUP Gleason score now ranges from 6 to 10, with lower scores frequently not needing direct treatment [11-13]. Importantly, in the ISUP 2014 consensus conference, a new type of classification was symbiotically introduced, the Group Grading (GG). The GG was first proposed in 2013, and created five prognostically distinct grade groups, based on the likelihood of PCa progression (***Table 1***). As the GG turned out as a more accurate prognosis method, the Modified ISUP Gleason

Score and GG have since then been coupled up to ensure the best overall disease prediction (***Figure 3***) [11].

***Table 1*. Characteristics of the five Group Gradings presented by ISUP.**

Category	Gleason Score	Associated Risk	Description
Grade Group 1	≤ 6	Very Low/Low	The tumor is well differentiated, more likely to grow more slowly, and less aggressive
Grade Group 2	7 (3+4)	Intermediate (Favorable)	The tumor is moderately differentiated, likely to grow (but without quick spread), and moderately aggressive
Grade Group 3	7 (4+3)	Intermediate (Unfavorable)	
Grade Group 4	8	High/Very High	The tumor is poorly differentiated, likely to grow and spread faster, and highly aggressive
Grade Group 5	≥ 9	High/Very High	

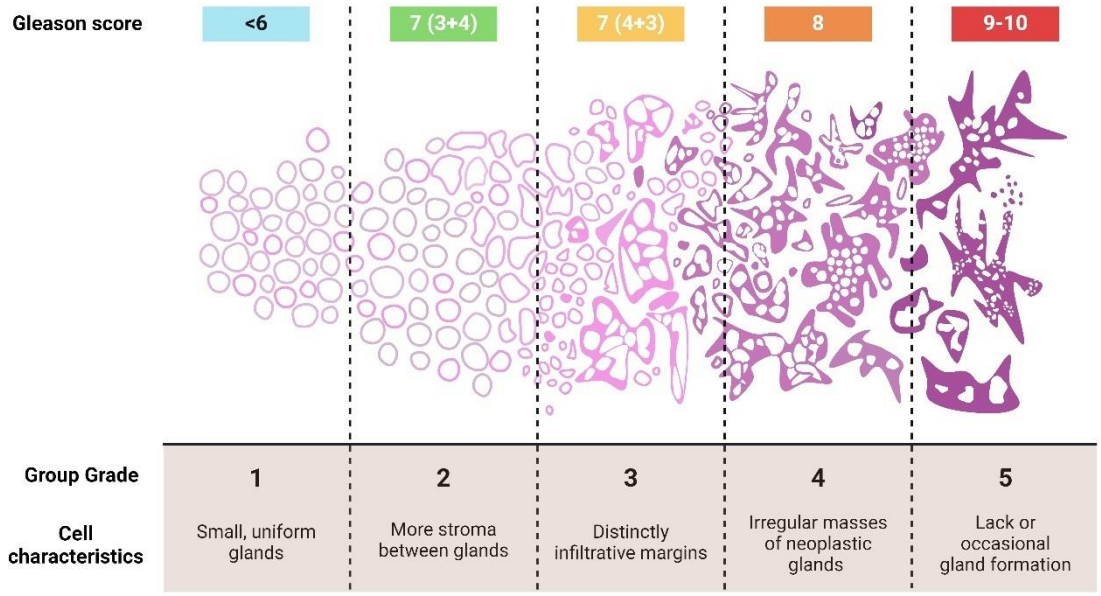

***Figure 3*. Histopathological characteristics of Gleason Score system associated with Group Grading.** Adapted from BioRender template with BioRender.com.

Diagnostic tools and treatment for prostate cancer

It has been known for a long time that PCa is a heterogeneous disease: although mostly organ-confined, PCa is often multifocal. This heterogeneity poses an obstacle for diagnosis and treatment of the patients, hence the need to have suitable diagnostic and treatment tools, as well as an adequate follow-up [14].

Currently, there are variate diagnostic tools available for PCa. The most known and primary test made for suspicion of PCa is the prostate specific antigen (PSA) test, an enzyme secreted by prostate epithelial cells. In most cases, values of PSA higher than 3.0 ng/mL are considered the threshold for PCa. However, this enzyme is not cancer specific, and abnormal levels may indicate other conditions, such as benign prostatic hyperplasia (BPH) or prostatitis (inflammation of the prostate) [15, 16]. Thus, another diagnostic tool was introduced: the prostate specific antigen density (PSA-D), which adjusts the PSA values according to the prostate volume, ensuring a better prediction in calculating risk. Nevertheless, PSA-D remains limited due to a lack of standardization in prostate volume categorization/definition/measurement. Additionally, other exams are available for risk assessment, such as digital rectal examination (DRE) and imaging techniques (magnetic resonance, ultrasound and tomography), as well as blood and urine specific biomarkers, including Prostate Health Index (PHI), 4K score and Prostate Cancer Gene 3 (PCA3) [15, 17, 18]. Globally, DRE associated with PSA test remains the most popular diagnostic techniques used for PCa detection [15].

Population-based screenings have been popular for identifying individuals who might be at risk of developing PCa. This type of screening is advised for men over 50 years of age, or younger men who have a family history of PCa, are of African descent or carry *BRCA2* gene mutations [15].

Regarding types of treatments for PCa, many options arise, according to the clinical needs of each patient. Radical prostatectomy has been a popular treatment and is currently mostly done in laparoscopic or robot-assisted surgery. Radiotherapy is also a very common technique used for PCa treatment, and can be delivered through external beam radiation, proton beam radiation or brachytherapy [15]. Most PCa cases (around 70-80% of total patients) are detected at initial stages and are still organ confined. In these cases, radiotherapy sessions or radical prostatectomy are the usual treatment approaches [19]. However, in other cases, localized PCa can evolve to CRPC, and hormone-dependent therapies are then used, where concomitant use of androgen deprivation therapy (ADT) and chemotherapy are usually the preferable methods [15, 19]. ADT is a type of hormonal therapy specifically used in PCa that binds directly and inhibits androgen receptors (AR), since the prostate is dependent on androgens for development and growth [20]. First line ADT consists of agonists or antagonists of gonadotropin-releasing hormone (GnRH), such as histrelin, goserelin, triptorelin, leuprolide and degarelix, which provide castration levels of testosterone for the patients [5, 20]. At the same time, chemotherapy is employed, where standard first line drug is docetaxel (with usual combination of corticosteroids), and second line treatment applies cabazitaxel or enzalutamide when docetaxel treatment is unsuccessful [5, 21].

Epithelial-Mesenchymal Transition

The cell phenotype difference between epithelial and mesenchymal cells is one of the most primordial divergences in organisms. Epithelial cells secure cell-cell cohesion, which is crucial for maintaining the integrity of multicellular organisms. They also act as a crucial barrier for regulating the internal environment independently from the external environment. On the other hand, mesenchymal cells offer support and structure to epithelial cells by producing an extracellular matrix. Unlike cells with epithelial phenotype, which are confined and immobile, mesenchymal cells present high motility and invasiveness [22].

These two different phenotypes are not static, depending on the environment and cell type. During embryogenesis, the conversion between epithelial to mesenchymal phenotypes – known as Epithelial-Mesenchymal Transition (EMT) – and the opposite conversion from mesenchymal to epithelial – the Mesenchymal-Epithelial Transition (MET) provides the flexibility needed for this process. Additionally, it facilitates wound healing, by allowing dynamic cellular remodeling of differentiated tissues [22].

Some of the most classical EMT-related proteins include E, P and N-Cadherin, ZO-1, Claudins, Snail, Slug, Vimentin and β-Catenin. E-Cadherin and P-Cadherin are associated with an epithelial phenotype, being responsible for cell-cell adhesion in epithelial cells [23, 24]. Similarly, Claudins and ZO-1 are epithelial-linked proteins, as they assemble into tight junctions between cells, enabling their adhesion [24-26]. On the other hand, Vimentin and β-Catenin are related with a mesenchymal phenotype. Vimentin acts as a facilitator for cell migration and invasion [27], whereas β-Catenin functions as a co-activator for the inhibition of E-Cadherin [26]. Similarly to β-Catenin, Snail and Slug are transcriptional repressors from the Snail family, and are responsible for binding to the E-Cadherin promoter, repressing its transcription and therefore inducing the EMT process [26]. With the repression of E-Cadherin, another protein is increased, N-cadherin, which is therefore associated with mesenchymal cells and phenotype [23, 26].

Although EMT is an essential process for organisms, this mechanism is also involved in diseases, such as cancer. The deregulation of transcription factors and pathways in EMT has been associated with cancer metastasis (***Figure 4***), and even presents as a hallmark of cancer [22, 28, 29]. In PCa, EMT is an important process, as it plays a crucial role in metastatic CRPC development. Several transcription factors and proteins related to EMT have been associated with PCa metastasis, such as Transforming Growth Factor Beta (TGF-β), Slug, β-Catenin, and E-cadherin, among others [30-33]. Therefore, understanding the regulation of EMT in this disease is crucial for its management.

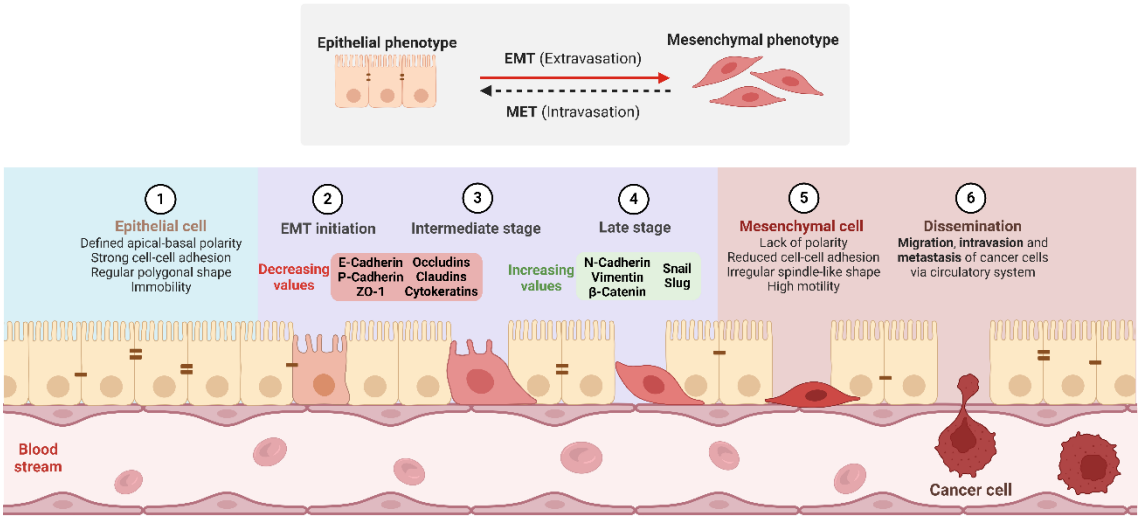

Figure 4. **Major transformations and characteristics of Epithelial-Mesenchymal Transition in cancer.** Information taken from [30-34]. Adapted from BioRender template with BioRender.com.

From Epigenetics to Epitranscriptomics: a new frontier in science

Epigenetics is considered an essential field of study in cancer. As a matter of fact, non-mutational epigenetic reprogramming is now considered a hallmark of cancer, indicating its importance in the transformation of normal cells to neoplastic [28]. The first definition of Epigenetics dates back to 1939 and comes from C.H. Waddington as "the branch of biology which studies the causal interactions between genes and their products, which bring the phenotype into being" [35]. As epigenetics evolved, the currently accepted definition is "the study of heritable changes in gene expression that occur independent of changes in the primary DNA sequence", and it is known that these changes are reversible [19, 36].

The main molecular mechanisms that enable epigenetic modifications are DNA methylation, histone post-translational modifications and non-coding RNA (ncRNA) (***Figure 5***). DNA methylation refers to the addition of methyl groups and occurs mostly in regions with a cytosine followed by a guanine, where higher concentrations of these clustered areas are named CpG islands [37]. Histone modifications are made through chemical processes, such as acetylation, methylation or phosphorylation, that occur normally in specific residues of lysine in histone tails [38]. Lastly, ncRNAs account for the vast majority of the human genome (around 98%), and are responsible for regulation of protein-coding RNAs [39]. ncRNAs can be divided according to its length: long ncRNAs (lncRNA) and small ncRNAs [40]. lncRNAs are longer than 200 nucleotides, and are responsible for the regulation of gene expression, translation, cell cycle and cellular differentiation. Inversely, small ncRNAs are shorter than 200 nucleotides, and can be further categorized in smaller groups, according to specific functions and length.

Alike to lncRNAs, small ncRNAs have important functions as regulators in a plethora of cellular mechanisms [41].

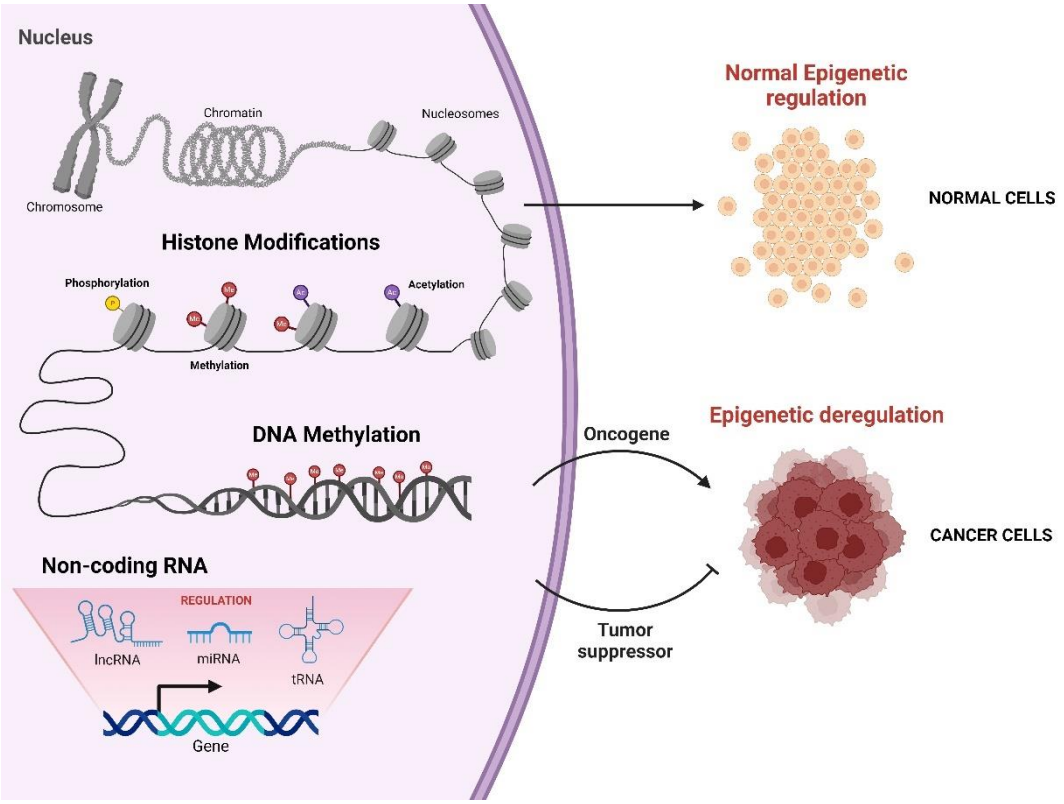

Figure 5. **Epigenetic mechanisms in the carcinogenic process.** Although these mechanisms are important in normal DNA regulation and modification, when deregulated can become enhancers for cancer cells proliferation and growth. Created with BioRender.com.

Historically, cancer was credited to be a genetic disease, so, naturally, the study of the genetic modifications that occurred in cancer – epigenetics – became a popular topic of interest. However, more recently, cancer has been recognized as a broader disease. Modifications do not occur exclusively in DNA, and over the past decade, extensive research efforts have been made to describe the functions, nature and biological tasks of RNA, revealing a new vital pillar in cell biology field – Epitranscriptomics [42, 43].

Epitranscriptomics refers to the study of reversible chemical modifications that occur in RNA molecules, including ncRNA and mRNA [43, 44]. These RNA modifications are responsible for the regulation of gene expression, such as oncogenes and tumor-suppressor genes. Thus, these alterations in the RNA are responsible for the promotion of cancer cell initiation and proliferation, as well as the regulation of invasiveness and potential for metastasis [45, 46].

Currently, more than 170 RNA modifications are known [42]. However, only a fraction of those were already subject of study, and some of the most known are N6-

Methyladenosine (m^6A), 5-Methylcytosine (m^5C), N1-Methyladenosine (m^1A), N7-Methylguanosine (m^7G), Pseudouridine (Ψ) (***Figure 6***), 5-Hydroxymethylcytosine (hm^5C) and 2'-O-Methylation (Nm). These RNA modification marks can range from simple methylations to more complex and multistep modifications [44, 45].

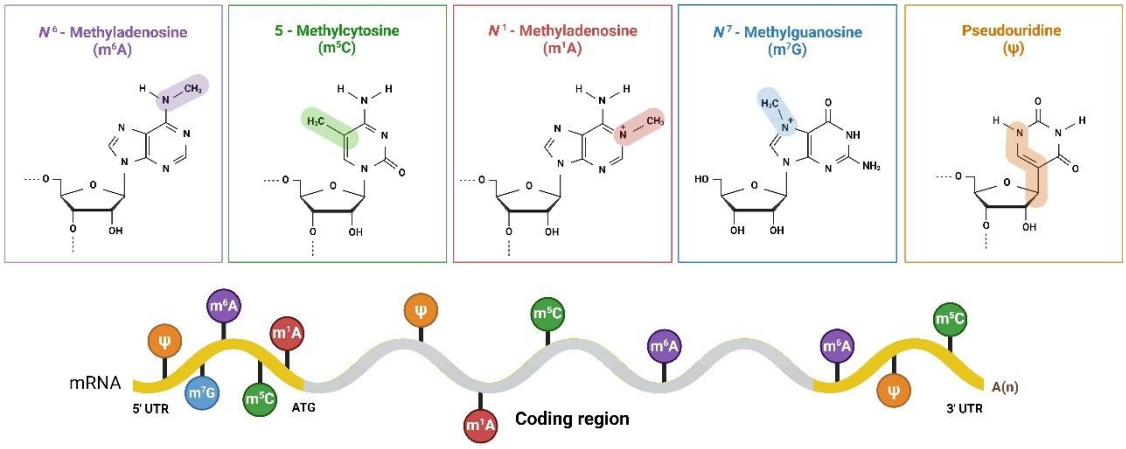

Figure 6. **Molecular configuration of the main epitranscriptomic marks and its known alteration sites in mRNA.** m^6A, m^5C, m^1A, m^7G and Ψ remain some of the most known RNA modifications, and can be found in all types of RNA. In mRNA, their location can vary from the coding region to the 5' and 3' ends. Information taken from [6, 7]. Created with BioRender.com.

Several types of proteins are responsible to promote changes in the RNA, and are known as RNA-Modifying Proteins (RMPs). These can be further categorized as one of three group: writers, erasers and readers. Writers are responsible for inserting the marks, whereas erasers are responsible for removing them. Readers are the proteins who selectively identify and bind to these alterations made by writers and erasers [42]. Deregulations in RMPs have been already connected with human diseases, such as cancer, obesity, neurological conditions and genetic defects [47].

The m^6A mark is by far the most studied, as it was the first RNA modification mark discovered, and is the most prevalent modified nucleotide found in mRNAs and in ncRNAs [42, 48]. However, the study of the m^5C mark has showed increasing importance, since it is present in several types of RNA, and is linked to leukemia, bladder, gastric, lung and gynecologic cancers, among others [43, 49, 50]. This will be the epitranscriptomic mark further studied for this project.

The 5-Methylcytosine RNA mark

The m^5C mark is an RNA chemical modification conserved in all life domains. It has a special interest in ncRNA, since it regulates RNA's structure, stability, and interaction with other molecules. Importantly, m^5C RNA modifications have been

linked with drug resistance and were already described as potential predictive biomarkers for treatment decision-making in cancer [51].

Specifically, m^5C regards a specific post-transcriptional modification that involves the addition of a methyl group to the fifth carbon of the cytosine base in RNA. All the players involved in this mark can be seen below (***Figure 7***). Additionally, since the writers add a methyl group in this mark, they are also called methyltransferases, and inversely, erasers can also be named demethylases [52].

Methyltransferases are the most described group of the m^5C regulatory network. It consists of the NOP2/SUN RNA Methyltransferase (NSUN) family and tRNA aspartic acid Methyltransferase 1 (TRDMT1), also known as DNA Methyltransferase 2 (DNMT2). The NSUN family is a group of proteins that recognize RNAs within aspartate side chains, and then target the specific cytosines. Currently, there have been identified 7 human NSUN variants: NSUN1 (also known as NOP2), NSUN2, NSUN3, NSUN4, NSUN5, NSUN6 and NSUN7. Lastly, contrary to its name, DNMT2 does not only methylate DNA, but also molecules of RNA, and, surprisingly, has a preference for specific binding to mRNA in detriment to DNA [50].

These methyltransferases can be found in the nucleus (NOP2, NSUN2, NSUN5 and TRDMT1), in the cytoplasm (NSUN2, NSUN6, NSUN7 and TRDMT1), and in the mitochondria (NSUN3 and NSUN4) [53]. Additionally, the NSUN family has been recognized as involved in m^5C methylation in mRNA, tRNA, rRNA, mtRNA, and even ncRNA, while TRDMT1 has been implied in tRNA methylation only [50]. More specifically, mRNA stability, translation and export from the nucleus is solely regulated by NSUN2, whereas tRNA cleavage and charging is controlled by NSUN2 and TRDMT1. Furthermore, ribosomal and mitochondrial assembly are regulated by NSUN2 and NSUN4, respectively, while NOP2, NSUN3, NSUN7 and TRDMT1 are responsible for transcription regulation [50, 53].

Next, the specific demethylases for m^5C RNA mark are the Ten-Eleven Translocation (TET) family, that consist of TET1, TET2 and TET3 [50]. These erasers work by mediating the base oxidation in m^5C, however, the mechanism used for this process is still not elucidated, as different theories are still proposed [50, 54]. Due to its function, these demethylases can be found all around the cell. Additionally, mRNA oxidation is regulated by TET1 and TET2, while the latter protein is also capable of regulating tRNA oxidation (therefore altering its fragments) [54, 55]. Mutations in TET2 have also been implied in hematologic malignancies, such as leukemia [55].

Lastly, the readers for m^5C are YTH Domain-containing Family 2 (YTHDF2), ALYREF Export Factor (ALYREF), and Y-box Binding Protein 1 (YBX1). Readers act as a type of barcode reader, which influences biological processes by recognizing and binding to m^5C sites [50, 54]. Additionally, YTHDF2 is a common reader between m^5C and m^6A RNA mark [56], and can be found in the cytoplasm and nucleus. ALYREF is only

present in the nucleus, while YBX1 is present in both sites, but is mainly located in the cytoplasm. In terms of functions, rRNA processing is regulated by YTHDF2, whereas ALYREF and YBX1 are responsible for mRNA stabilization and shuttling from the nucleus to cytoplasm [50, 54]. However, little is still known about these readers, and further investigation of novel specific binding proteins might be needed [50].

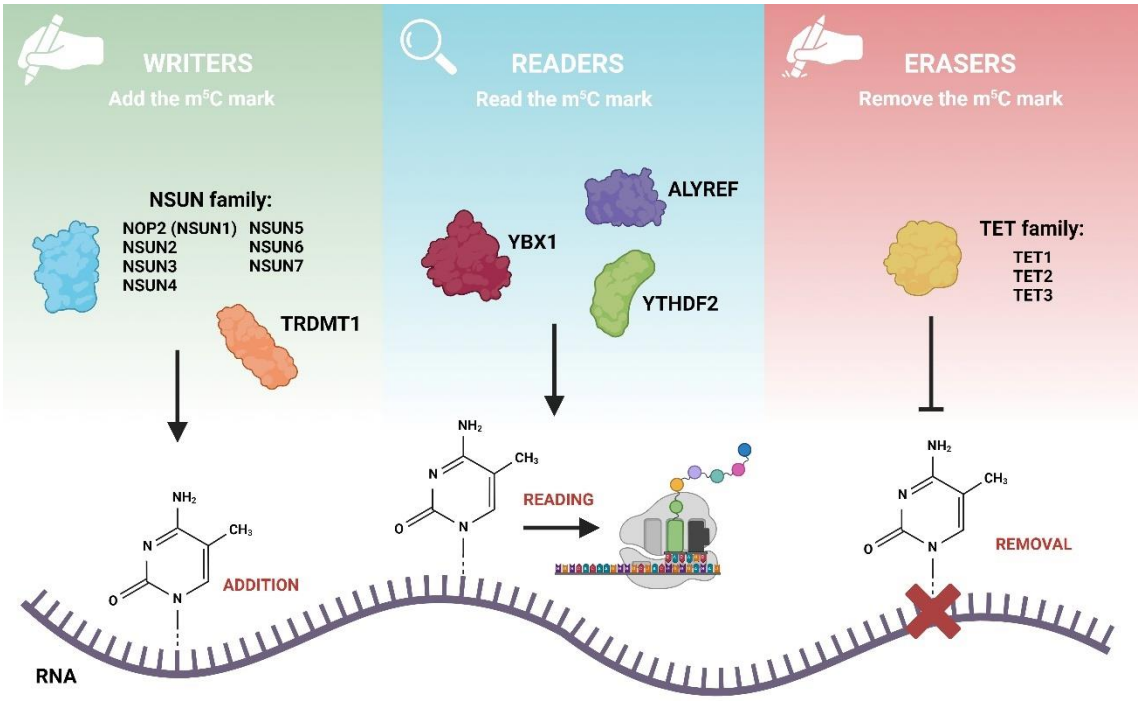

Figure 7. **Effectors of RNA m^{5}C, divided by its function.** Writers (or methyltransferases) are responsible for the addition of the m^{5}C mark, whereas erasers (or demethylases) remove these marks. Readers are the proteins capable of reading all these alterations made in the RNA. Created with BioRender.com.

AIMS

Aims

Epitranscriptomics has emerged as a key field of study in oncology, shedding light on the dynamic modifications of RNA and its impact on gene expression and cellular function in tumor development. Much is now known about the link between epitranscriptomics and cancer, especially in m^6A, that is currently associated with the development of a plethora of diseases, such as prostate, ovarian, lung, bladder and breast cancers, between many others [57-62]. However, the main functions of m^5C, specifically in PCa, remain unknown.

With this in mind, the main aim of this Master's Dissertation is to comprehensively characterize the m^5C mark in PCa, and understand its importance in functional and regulatory networks. More specifically, this project is divided into three major sections:

Aim 1: Profiling of m^5C regulators in PCa samples.

Aim 2: Assess m^5C regulators' expression in PCa cell lines.

Aim 3: Dissecting the role of the most aberrantly altered m^5C regulator in PCa development.

MATERIALS & METHODS

In silico analysis

An *in silico* analysis was conducted to assess the mRNA expression levels of different m^5C players: *NSUN1* to *7*, *TRDMT1*, *YBX1*, *YTHDF2*, *ALYREF*, and *TET1* to *3*. The Cancer Genome Atlas (TCGA) database for PCa, comprising 492 PCa samples and 52 normal prostate samples was used for *in silico* analysis through the Gene Expression Profiling Interactive Analysis (GEPIA) web server platform and cBioPortal for Cancer Genomics.

The cBioPortal for Cancer Genomics was selected to determine the frequency of gene alterations in all m^5C players. The standard processing pipeline used for m^5C players expression analysis is: $|Log_2FC|$ Cutoff=0.05, *p*-value cutoff=0.01 [63].

Patients' selection and sample collection

Fresh frozen tissues from an independent cohort of 45 patients with PCa submitted to radical prostatectomy at the Portuguese Oncology Institute of Porto (IPO Porto) between 2001 and 2005 were selected. The patients were divided by ISUP GG: 10 patients from GG1, 10 patients from GG2, 10 patients from GG3, 5 patients from GG4, and 10 patients from GG5. A matching set of 45 formalin-fixed and paraffin-embedded tissues was retrieved from the archives of the Department of Pathology at IPO Porto. Normal prostate formalin-fixed and paraffin-embedded tissue from 10 patients submitted to cystoprostatectomy (CP) due to bladder cancer were also used for control purposes. Clinical-pathological characteristics from the PCa patients, as well as the 10 CP patients used for control purposes, can be seen in the table below (***Table 2***).

All the clinical files and pathology reports were thoroughly reviewed. Additionally, all histological slides were reviewed by a pathologist, and tumors were classified in consideration of the most recent criteria [64]. This study was approved by the Ethics Committee (Comissão de Ética para a Saúde) of IPO Porto (CES-IPO nº 2016.019).

Table 2. **Clinical and pathological features of PCa and CP patients' cohort.**

Patients		Nº of cases	Median age at diagnosis	Median PSA at diagnosis (ng/mL)	Diagnosis method (%)		Clinical recurrence (%)		Pathological stage (%)			
					PSA	Biopsy	No	Yes	pT2a	pT2b	pT3a	pT3b
Localized PCa	GG1	10	60 years (51 – 66)	12.39 (6 – 20)	1 (10%)	5 (50%)	9 (90%)	1 (10%)	0	1 (10%)	7 (70%)	2 (20%)
	GG2	10	64.7 years (53 – 68)	10.89 (7.43 – 15)	0	4 (40%)	8 (80%)	2 (20%)	0	3 (30%)	7 (70%)	0
	GG3	10	62.9 years (51 – 71)	10.61 (3.5 – 17.7)	0	5 (50%)	9 (90%)	1 (10%)	0	4 (40%)	2 (20%)	4 (40%)
	GG4	5	62.7 years (60 – 66)	8.90 (4.03 – 15)	0	1 (20%)	4 (80%)	1 (20%)	1 (20%)	0	2 (40%)	2 (40%)
	GG5	10	62.6 years (52 – 69)	11.80 (6.23 – 19.87)	0	1 (20%)	4 (40%)	6 (60%)	0	0	4 (40%)	6 (60%)
CP		10	68,9 years (54 – 80)	n.a.	n.a.		n.a.		n.a.			

n.a. – Non applicable.

RNA extraction and cDNA synthesis

RNA was extracted from various prostate cell lines with the use of TRIzol reagent (Thermo Scientific Inc., USA) (***Figure 8***). In this procedure, the cell flask was washed with phosphate buffered saline (PBS) 1x, and 1 mL of TRIzol was added. Then, the cells were scraped, and the mixture was transferred to a tube and let homogenize for 5 min at room temperature. Next, 200 µL of chloroform was added, and left to homogenize for 2 min. After a centrifugation at 10000 RPM for 15 min at 4 ºC, three phases were created: an organic phase at the base, with a reddish color and consisting of proteins and lipids from the cells, an interphase, containing DNA, and an aqueous phase at the top, containing the total RNA from the cells. The aqueous phase was transferred to a new RNAse-free tube, and 500 µL of isopropanol was added for 5 min at room temperature to RNA precipitation, following centrifugation for 10 min at 4 ºC. Then, the supernatant was discarded, and the RNA was washed twice with 1 mL of ethanol 75% and centrifuged at 10000 RPM for 5 min at 4 ºC. Finally, the supernatant was discarded, the tubes were left upside down for 30 min to evaporate the remaining ethanol, and the RNA was resuspended with 10 µL of bidistilled water and stored for longer periods of time at -80 ºC.

For the complementary DNA (cDNA) synthesis from the extracted RNA, a previous RNA quantification was done using the NanoDrop Spectrophotometry System (Thermo Scientific Inc., USA). This system measures the absorbance of RNA at a wavelength of 260 nm (A260). The analysis was made with 1 µL of bidistilled water as a blank, and 1 µL of RNA was used to measure concentration and purity. Ideal samples have a concentration between 100 – 1000 ng/µL, and a A260/A280 purity

ratio of approximately 2. Higher or lower than 2 purity ratios are suggestive of DNA, protein or phenols contamination.

Regarding the cDNA synthesis itself, the kit used to transform the RNA into cDNA was RevertAid First Strand cDNA Synthesis Kit (Thermo Scientific Inc., USA) (***Figure 9***), because it uses an appropriate transcriptase, presenting a lower RNase H activity in comparison with other reverse transcriptases (RT), such as Avian Myeloblastosis Virus (AMV).

Firstly, proper dilutions of each sample were made, according to its concentration, for a quantity of 1000 ng in a volume of 11 µL. Then, 1 µL of random hexamer primers were added to each tube, transferred to a Veriti thermocycler (Thermo Scientific Inc., USA), and put in a program of 65 ºC for 5 min. Next, 8 µL of a mix of RiboLock RNase inhibitor, dNTPs at 10 nM, 5x Reaction buffer and RevertAid RT enzyme was added to the tubes, prefacing a total volume of 20 µL. Lastly, the tubes were put to a program in the thermocycler of 5 min at 25 ºC, 60 min at 42 ºC, and 5 min at 70 ºC, for the final conversion into cDNA. The storage was made at -20 ºC.

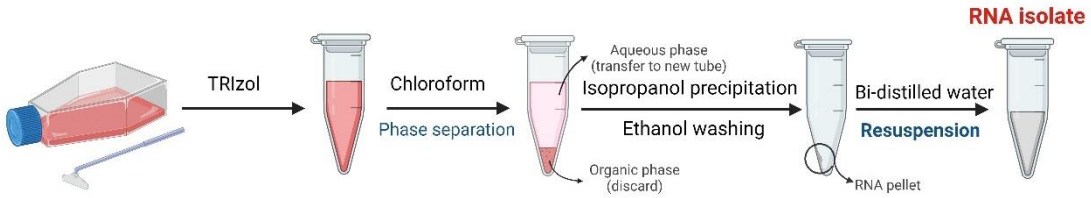

Figure 8. **Basic steps of RNA extraction assay.** Created with BioRender.com.

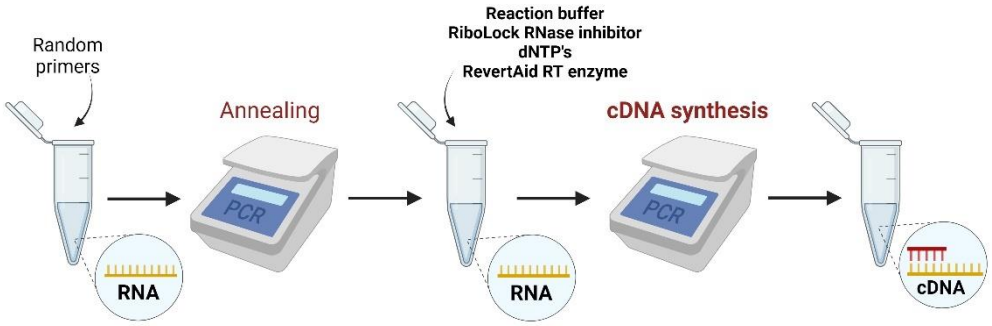

Figure 9. **Basic steps of cDNA synthesis assay.** Created with BioRender.com.

Reverse Transcriptase Quantitative PCR

Following the cDNA synthesis from RNA extracted from cell lines, Reverse transcriptase quantitative PCR (RT-qPCR) was performed in these samples, as well as in the described fresh frozen PCa cohort.

In this process, cDNA at 5 ng/µL was combined with Xpert Fast SYBR (GRiSP, Porto, Portugal) (with 4 µL of ROX per vial previously added) and primers mix (forward and reverse) at 10 µM, totaling a final volume of 10 µL per reaction well. Every sample was made in triplicates, to ensure curve efficiency, and positive and negative controls were used to each primer employed, to confirm its quality. After adding the cDNA, SYBR and primers, the 384-well PCR plates were sealed and centrifuged at 1000 RPM for 1 min at room temperature. Lastly, the plates were transferred to the Real-Time PCR (RT-PCR) thermocycler QuantStudio 12K Flex (Applied Biosystems, Thermo Scientific Inc., USA), and put to a specific temperature (ranging from a temperature of annealing of 60 ºC to 66 ºC) and cycle program (ranging from 40 cycles to 45 cycles), according to each primer. The forward and reverse sequences, as well as annealing temperature of each primer can be seen below (***Table 3***).

Table 3. **Characteristics of primers used in RT-qPCR.**

Gene	Foward Sequence (5' – 3')	Reverse Sequence (3' – 5')	Annealing Temperature
TPJ1	TGGATTTACCTGTCAGTCCATCT	CAGCCGCAACCCACACTAT	60 ºC
CDH II	AGGCTTCTGGTGAAATCGCA	GCAGTTGCTAAACTTCACATTGAG	64 ºC
CDH I	CTTTGACGCCGAGAGCTACA	AAATTCACTCTGCCCAGGACG	64 ºC
CDH III	GAGGAGATTGCCAAGTATGAGC	GTCACGATGATGGAGATGTTCA	66 ºC
CTNNB1	AGGGCTTACTGGCCATCTTT	AAGGTTGTGGAGAGTTGTAATGG	64 ºC
VIM	CGAAAACACCCTGCAATCTT	CTGGATTTCCTCTTCGTGGA	60 ºC
SNAI2	TGGTTGCTTCAAGGACACAT	GCAAATGCTCTGTTGCAGTG	60 ºC
SNAI1	CCCAATCGGAAGCCTAACTA	GGACAGAGTCCCAGATGAGC	64 ºC
CLDN1	GATGAGGTGCAGAAGATGAGGAT	GACTGGGGTCATAGGGTCATAGAAT	60 ºC
GUSB	CACTGAAGAGTACCAGAAAAGTC	TCTCTGCCGAGTGAAGATCC	60 ºC-66 ºC*
YTHDF2	GGAGCAGAGACCAAAAGGTCA	GCATTATTGGGCCTTGCCTG	60 ºC
NOP2	GGAGATTGGGCTCTGTTGAAG	AGCTCCTTTTGGTAGCTTTCC	60 ºC
NSUN2	GAACTTGCCTGGCACACAAAT	TGCTAACAGCTTCTTGACGACTA	60 ºC
NSUN6	TCTCAGCCCTTCATTTGACAGT	TCCAGTGCTATAACTTCTCCCTG	60 ºC

*The sequence of *GUSB* primer can handle different temperatures of annealing, ranging from 60 ºC to 66 ºC.

Immunohistochemistry

Immunohistochemistry (IHC) was performed in slides from the matched samples of PCa patients submitted to prostatectomy at IPO Porto. The levels of the reader

NSUN2 were evaluated in patients' tissues using the Novolink Max Polymer Detection System (LeicaBio systems, Germany) (**Erro! A origem da referência não foi encontrada.**). Colon tumor tissue was used as IHC positive control for NSUN2 expression. Several optimizations were made to achieve ideal IHC efficacy.

Thick sections of 4 µm were cut using a micrometer and placed in coated slides. To help the paraffin melting, the slides were put in an oven at 60 ºC for at least 15 min. Subsequently, the slides were deparaffinated, with two baths of xylene for 10 min each, and hydrated in ethanol baths with decreasing concentrations: two baths at 100% for 5 min each, and 95%, 90% and 70% baths for 3 min each, respectively. After a 3 min wash in running water, antigen retrieval was attained in ethylenediamine tetraacetic acid (EDTA) buffer pH=8 (Abcam, Cambridge, UK) in the microwave for 25 min at 800 W, followed by 20 min of cooling. Then, the tissues were delimited by a hydrophobic pen, and the slides were put in a wet chamber and the endogenous peroxidase activity was then inhibited with hydrogen peroxide solution at 3% in methanol, for 10 minutes. Next, the slides were washed with tris-buffered saline solution with Tween 20 (TBS-T) at 0.1%, and any unspecific binding was blocked with horse serum at a 1:50 dilution with antibody diluent for 20 min. Lastly, the slides were washed again in TBS-T at 0.1%, and the incubation of the NSUN2 primary antibody (1:400 dilution) (#52901, Cell Signaling) was performed overnight at 4 ºC.

The next day, all slides were washed with TBS-T at 0.1%, and incubated with post primary for 30 min, followed by polymer for 30 min. The slides were then washed again with TBS-T, followed with PBS 1x, and signal was developed with 3,3'-Diaminobenzidine tetrahydrocloride cromogen (DAB) (Sigma-Aldrich, Germany) for 10 min and counterstained with filtered hematoxylin. Next, the slides were washed with warm water to allow nucleus differentiation, and dehydration and diaphanization was performed, in an opposite order from the beginning: ethanol baths at 70%, 90% and 95% for 3 min each, respectively, and two baths at 100% for 5 min each, followed by two baths of xylene for 10 min each. Finally, the slides were mounted in a Leica CV5030 glass coverslipper (Leica Biosystems, Germany).

Lastly, an experienced pathologist performed a semi-quantitative analysis of the protein expression, by categorizing the slides according to intensity and overall percentage. The intensity score was applied as 0 if immunostaining was absent, 1+ if it was less intense than the control tissues, 2+ when with similar intensity to the control tissues, and 3+ if it presented more intensity than the control tissues. Additionally, the percentage score was classified as 0 if less than 1% of cells were immunoreactive, 1+ for up to 30% of immunoreactive cells, 2+ for 30 to 70% of immunoreactive cells, and lastly 3+ for 70 to 100% of immunoreactive cells. The final IHC scoring was calculated with the multiplication of the intensity score with the percentage score, therefore ranging from 0 to 9+. Pictures were taken in a

microscope Olympus BX41 with a digital camera Olympus U-TV0.63XC (Olympus Corporation, Japan) using Applied Spectral Imaging software (ASI Ltd., Israel).

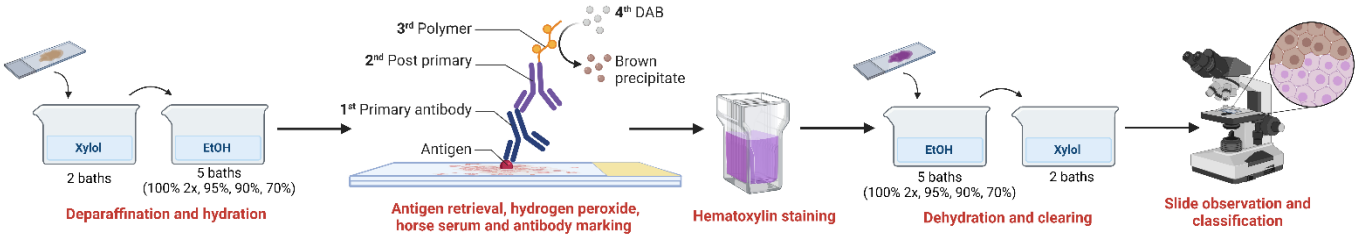

***Figure 10.* Basic steps of an IHC assay**. Created with BioRender.com.

Prostate cell lines

Seven PCa cell lines, 22Rv1, LNCaP, C4-2, C4-2B, PC-3 and Du145 were used for the characterization of m^5C players, as well as one normal prostate epithelium cell line, RWPE-1, and one non-malignant prostate epithelium cell line, PNT2. The cell lines' characteristics can be seen in the table below (***Table 4***).

The RPMI 1640 culture media was supplemented with 10% Fetal Bovine Serum (FBS) (Biochrom, Merck, Germany) and 1% penicillin/streptomycin (GIBCO, Invitrogen, USA), providing the cells with a complete culture media (RPMIc). The cells were maintained in an incubator at 37 ºC and 5% CO_2. Additionally, all cells were frequently tested for *Mycoplasma spp.*, using TaKaRa PCR-based Mycoplasma detection kit (TaKaRa Bio Inc., Shiga, Japan).

***Table 4.* Characteristics of the prostate cell lines used.**

Name	Cell Type	Patient Source	Androgen Receptor	Origin	Culture Media
PNT2	Non-Malignant Epithelium	33 year-old male	Positive	n.a.	RPMIc
RWPE-1	Normal Epithelium	54 year-old male, Caucasian	Positive	n.a.	K-SFM
22Rv1	Tumour	Male with Gleason score 9 PCa	Positive	Derived from xenograft of CWR22R cells	RPMIc
LNCaP	Tumour	50 year-old male, Caucasian	Positive	Lymph Node metastasis	RPMIc
C4-2	Tumour	n.a.	Positive	Chimeric tumor from LNCaP and human fibroblasts	RPMIc
C4-2B	Tumour	n.a.	Negative	Bone metastasis from C4-2	RPMIc
PC-3	Tumour	62 year-old male, Caucasian	Negative	Bone metastasis	RPMIc
Du145	Tumour	69 year-old male, Caucasian	Negative	Brain metastasis	RPMIc

n.a. – Non applicable.

Protein extraction and quantification

Total protein was extracted from the different PCa and normal/non-malignant cell lines in culture. For this, cells were collected from cell culture flasks and homogenized in Radioimmunoprecipitation Assay (RIPA) lysis buffer (Santa Cruz Biotechnology Inc., USA) supplemented with 10% Protease inhibitor Cocktail (PIC) 10x (Merck, Germany). The samples were put in ice for 15 min and were subsequently centrifuged at 13000 RPM for 30 min at 4 ºC. After the centrifugation, the supernatant was collected into a different tube.

Then, protein quantification was made using a Pierce BCA Protein Assay Kit (Thermo Scientific Inc., USA), according to the manufacturer's instructions.

Western Blot

Western Blot was employed to identify and quantify specific proteins from PCa and normal/non-malignant cell lines (***Figure 11***). Firstly, 3.2 µL of loading buffer was added to 20 µg of total protein from the different cell lines, previously diluted in water, and put at 95 ºC for 5 min to denature its structures. Then, after being put on ice and centrifuged, the samples were loaded in a polyacrylamide gel (with 8-12% concentration, depending on the type of molecular weight separation desired), and separated by molecular weight through a sodium dodecyl sulphate-polyacrylamide gel electrophoresis (SDS-PAGE) system at 100 V for 1 h 30 min at room temperature. The proteins in the gel were then transferred to a 0.22 µm WesternBright nitrocellulose membrane (Advansta Inc., USA), using a Tris-base/glycine 25mM buffer and two different transfer systems, according to specific protein needs: a semi-dry transfer with Trans-Blot Turbo Transfer system (Bio-Rad Laboratories, Inc., CA, USA) at 25 V and 1.3 mA for 20 min; or a wet transfer with a Tank Blotting system (Bio-Rad Laboratories, Inc., CA, USA) at 50 V and 1.3 A for 1 h at 4 ºC. After the transfer, the membranes were blocked with 5% dry milk in TBS-T, for 1 h at room temperature, followed by an incubation with primary antibody (***Table 5***) overnight at 4 ºC with agitation. The next day, the membranes were washed with TBS-T 3 x 5 min with agitation, and incubated with the respective secondary antibody (Cell Signaling Technology) for 1 h at room temperature (***Table 5***). Finally, the membranes were washed with TBS-T 3 x 5 min with agitation, incubated with Enhanced Chemiluminescence (ECL) (Bio-Rad Laboratories, Inc., CA, USA), and revealed with a ChemiDoc Imaging System (Bio-Rad Laboratories, Inc., CA, USA). Additionally, β-Actin was used as loading control, and quantification was made by band densitometry analysis using ImageJ Software version 1.8.0 (National Institutes of Health, USA).

***Table 5.* Characteristics of primary antibodies used in Western Blot.**

Antibody	Manufacturer	Molecular Weight	Dilution	Incubation time	Secondary antibody
Anti-ZO-1	Cell Signaling (#8193)	220 KDa	1:750	Overnight	Anti-rabbit
Anti-E-Caderin	BD Transduction Laboratories (#C20820)	120 KDa	1:300	Overnight	Anti-mouse
Anti-β-Catenin	Cell Signaling (#8480)	92 KDa	1:1000	Overnight	Anti-rabbit
Anti-Vimentin	Cell Signaling (#5741)	57 KDa	1:1000	Overnight	Anti-rabbit
Anti-β-Actin	Sigma-Aldrich (#A1978)	42 KDa	1:10 000	1 hour	Anti-mouse
Anti-SLUG	Cell Signaling (#9585)	30 KDa	1:750	Overnight	Anti-rabbit
Anti-SNAIL	Cell Signaling (#3879)	29 KDa	1:750	Overnight	Anti-rabbit
Anti-Claudins	Cell Signaling (#13255)	20 KDa	1:1000	Overnight	Anti-rabbit
Anti-NOP2	Cell Signaling (#90709)	110 KDa	1:500	Overnight	Anti-rabbit
Anti-NSUN2	Cell Signaling (#52901)	100 KDa	1:500	Overnight	Anti-rabbit
Anti-5-Methylcytosine	Active Motif (#39649)	n.a.	1:2000	Overnight	Anti-mouse

n.a. – Non applicable.

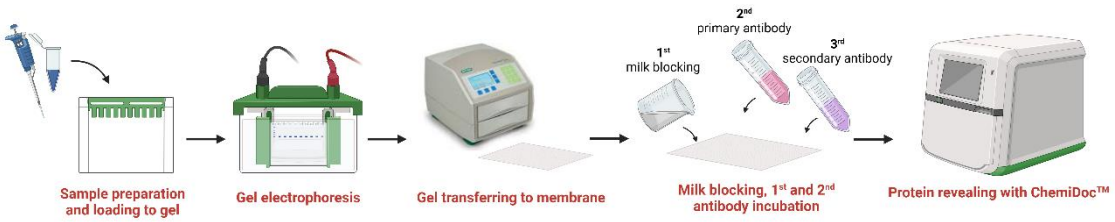

***Figure 11.* Basic steps of Western Blot assay.** Created with BioRender.com.

NSUN2 silencing via short hairpin RNA transduction

NSUN2 knockdown was performed in the C4-2B cell line via short hairpin RNA (shRNA) transduction, because it offers a highly efficient and stable knockdown for the desired gene.

The transduction was made with Dharmacon GIPZ Lentiviral shRNA vectors (Horizon Discovery, Cambridge, United Kingdom), which consists of three shRNA constructs targeting the human NSUN2 gene, one non-silencing control (negative

control), and one Glyceraldehyde 3-phosphate dehydrogenase (GAPDH) positive control, to control experimental workflow (***Table 6***). All these vectors include a Turbo Green Fluorescent Protein (TurboGFP) marker for the cells that incorporated the shRNA. To ensure high efficiency of the protocol, transduction conditions were optimized, such as the value of multiplicity of infection (MOI). MOI defines as the number of viral transducing units per cell, and can be influenced by several factors, such as the nature of the cell, the nature of the gene of interest, and the transduction efficiency. According to the conditions of this study, MOI 10 and MOI 20 were chosen to test optimal transduction efficiency. The volume of shRNA vector to pipette for each MOI can by calculated by:

1) nº cells per well x MOI = y **2)** $\frac{y}{\text{Titer (TU/mL)}} = \text{Volume (µL)}$

***Table 6*. Characteristics of Dharmacon GIPZ Lentiviral shRNA vectors.**

Name	Source Clone ID	Gene Target Sequence	Titer (TU/mL)
Non-silencing shRNA negative control	n.a.	n.a.	3.94×10^8
GAPDH shRNA positive control	n.a.	n.a.	9.87×10^8
Sh I	V2LHS_173635	CACACAAATTTAAGTCGAA	6.45×10^8
Sh II	V3LHS_311369	AGGAACTGGTGACACAGAA	1.05×10^9
Sh III	V3LHS_311366	AAGCTGTTCGAGCACTACT	8.62×10^8

n.a. – Non applicable.

Briefly, 3×10^4 cells/well were plated in 24-well plates and incubated overnight. Then, on the next day, the culture media was removed, and a new media with the adequate amount of lentiviral shRNA per MOI conditions tested (MOI 10 and MOI 20) was added to the wells, and the cells were incubated again at 37 ºC and 5% CO_2. At the timepoint of 48 h post-transduction, the wells were observed with the Olympus IX51 Inverted Fluorescence microscope (Olympus Corporation, Japan) with a digital camera Olympus XM10 (Olympus Corporation, Japan) in a Fluorescein Isothiocyanate (FITC) filter, for the presence of the reporter gene TurboGFP expression. The presence of TurboGFP in the cells is the first indicator that the transduction was successful, suggesting that the vector was able to be incorporated in the cells.

With the intent to reduce background expression of the gene from untransduced cells, a selection of puromycin was made. This protocol works by killing the cells that did not incorporate the shRNA vector, as the vector includes a puromycin

resistance. First, the same cell density for the transduction was used for platting the wild type cells, with RPMI, in 24-well plates. The next day, the culture media was replaced with different puromycin concentrations (ranging from 0.25 – 2.0 µg/mL). The cells were then observed daily and photos were taken for the next 7 days, and the culture media was replaced as needed. After the 7 days, a puromycin curve was made, and the minimal concentration of antibiotic that kills efficiently all puromycin-sensitive cells was identified, at 1.0 µg/mL. Lastly, this concentration of puromycin was used on the vials of all the 3 shRNA transduced cells and negative control, and the cells were carefully watched in the following 7 days, observing the percentage of surviving cells and its TurboGFP gene expression with FITC filter. At the end of the selection process, all media with puromycin was taken off, and replaced with the usual RPMIc without other reagent additions.

Once the puromycin selection was complete and the transduced cell line was stable, the percentage of NSUN2 silencing was assessed, using RT-qPCR and Western Blot analysis.

Dot Blot

The Dot Blot technique was employed to evaluate the relative quantity of m^5C mark in total RNA from the different PCa and normal/non-malignant cell lines (***Figure 12***). For this, specific quantities of RNA were diluted in bidistilled water, and, to undo the secondary structures, the samples were incubated at 95 ºC for 3 min, before being put in ice immediately. Then, drops of 2 µL of diluted RNA were put in 0.45 µm Amersham Protran nitrocellulose membranes (Merck, Germany), and put under UV light for 5 min, to allow cross-linking. Next, the membranes were washed with TBS-T for 5 min with agitation and blocked with 5% dry milk in TBS-T for 1h at room temperature, followed by m^5C antibody (***Table 5***) incubation overnight at 4 ºC. The next day, the membranes were washed with TBS-T for 3 x 5 min with agitation and incubated in secondary antibody for 1 h at room temperature. Lastly, the membranes were washed with TBS-T 3 x 5 min with agitation, and incubated with ECL (Bio-Rad Laboratories, Inc., CA, USA), and revealed with a ChemiDoc Imaging System (Bio-Rad Laboratories, Inc., CA, USA). As a loading control, the membranes were incubated with methylene blue staining buffer 0.2% for 30 min with agitation and photos were taken.

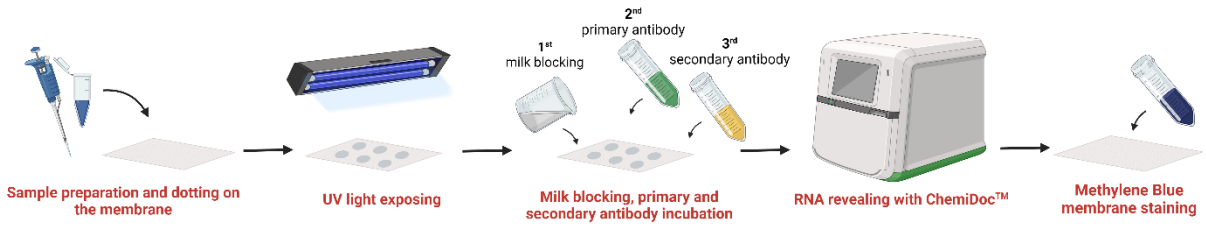

Figure 12. **Basic steps of Dot Blot assay.** Created with BioRender.com.

Statistical analysis

The statistical analysis was performed with the use of GraphPad Prism Software version 8.0.2 (GraphPad Software, CA, USA) and SPSS Statistic Software version 26 (IBM-SPSS Inc., CA, USA). For two-group comparisons, non-parametric Mann-Whitney U test was performed, whereas for multiple-group comparisons, non-parametric Kruskal-Wallis test was employed. For categorical data group comparisons, such as IHC analysis, Chi-square or Fisher's exact test was utilized.

P-values were considered statistically significant when inferior to 0.05. The significance is presented in comparison with the respective control and/or other groups, and is depicted as it follows: *$p \leq 0.05$; **$p < 0.01$; ***$p < 0.001$; ****$p < 0.0001$ and $^{ns}p > 0.05$ (non-significant).

RESULTS

In silico analysis of m^5C players

An *in silico* analysis was made for all the m^5C-related writers, readers and erasers, using normal prostate and prostate adenocarcinoma (PRAD), from the TGCA database. The analysis showed significantly higher levels of writers *NOP2*, *NSUN2*, *NSUN5*, *NSUN6*, and *NSUN7* (***Figure 13 A.***) and erasers *TET2* and *TET3* (***Figure 13 C.***) in PCa than in normal tissues. Additionally, although not significant, the same tendency was found for reader *YTHDF2* (***Figure 13 B.***). In fact, NSUN2, the major m^5C writer, followed by NSUN6 [65] was reported to associate with rapid PCa progression [66]. Furthermore, NOP2 increased expression was considered an indicator of poor prognosis in PCa, associated with PSA levels, Gleason score, and recurrence, by prompting EMT initiation [67]. Then, YTHDF2 was previously identified as highly expressed in PCa, also correlating with poor prognosis, by acting as a facilitator of proliferation and migration [68], as well as associated with progression of other cancers like leukemia, bladder, cervical, lung, and colorectal cancers [69]. Thus, YTHDF2, NOP2, NSUN2, and NSUN6 were selected for further analysis in patients' samples.

Nonetheless, the frequency of genetic alterations in these m^5C effectors was rather low (up to 3%), with most percentages lower than 1%, suggesting that genetic alterations are quite rare in this tumor type, while epitranscriptomic alterations in the m^5C effectors may be relevant (***Supplementary Figure 1***).

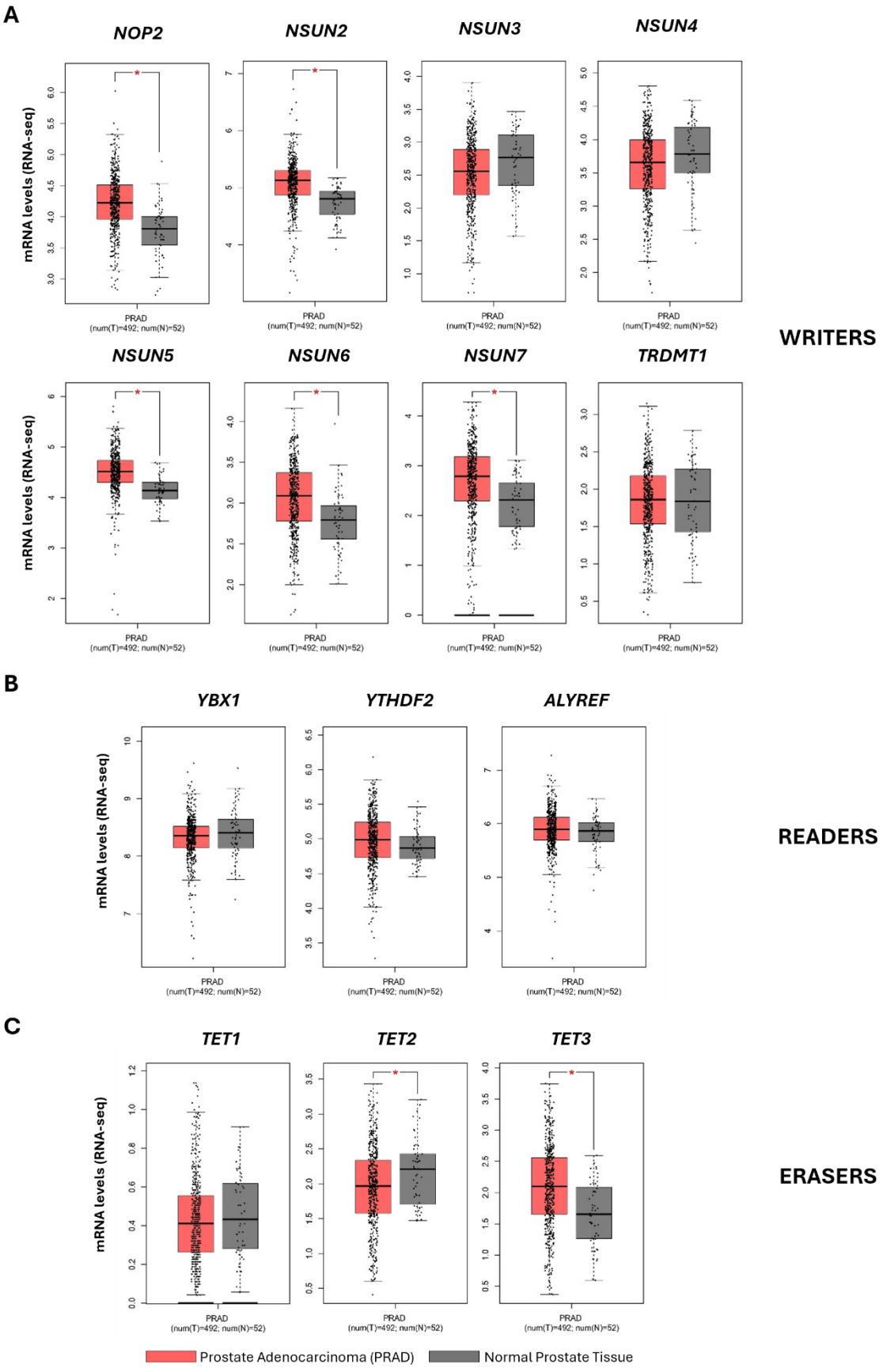

Figure 13. **m^{5}C modifying enzymes expression analysis in prostate adenocarcinoma and normal prostate.** From TCGA database, where n=492 for tumor (T), and n=52 for normal (N). **A.** Writers from *NSUN* family (*NOP2*-*NSUN7*) and *TRDMT1*. **B.** Readers *YBX1*, *YTHDF2* and *ALYREF*. **C.** Erasers from *TET* family (*TET1-3*).

Evaluation of selected m^{5}C players in IPO Porto PCa patients' samples through qPCR

YTHDF2, *NOP2*, *NSUN2*, and *NSUN6* transcript levels players were evaluated and displayed by GG. The results show that higher GG (GG3+GG4+GG5), and less differentiated PCa samples displayed significantly higher *NSUN2* transcript levels than lower GG (GG1+GG2) (***Figure 14 C.***), while no associations were found for *YTHDF2*, *NOP2* and *NSUN6* and tumors differentiation (***Figure 14 A.***, ***B.*** and ***D.***).

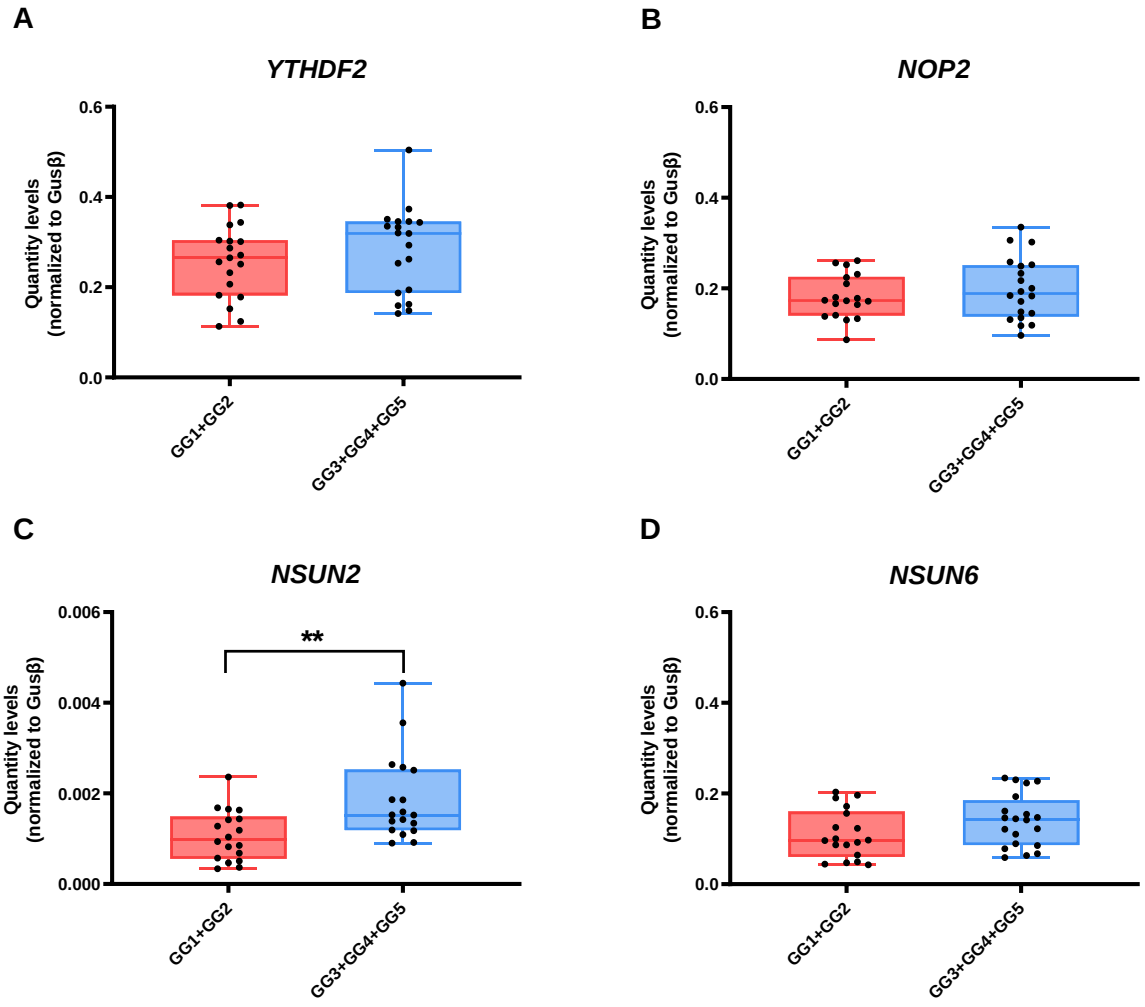

Figure 14. **Transcript levels of *YTHDF2*, *NOP2*, *NSUN2* and *NSUN6* in PCa patients, categorized by GG.** Results grouped by lower GG (1+2) and higher GG (3+4+5). All transcript levels were normalized to a housekeeping gene (Gusβ). Statistics from Mann-Whitney tests, where *p<0.05, **p<0.01, ***p<0.001 and ****p<0.0001. **A.** *YTHDF2* levels (GG1+GG2 n=19; GG3+GG4+GG5 n=19). **B.** *NOP2* levels (GG1+GG2 n=18; GG3+GG4+GG5 n=20). **C.** *NSUN2* levels (GG1+GG2 n=18; GG3+GG4+GG5 n=18). **D.** *NSUN6* levels (GG1+GG2 n=18; GG3+GG4+GG5 n=20).

Additionally, significantly higher YTHDF2, NSUN2 and NSUN6 transcript levels were found in PCa at more advanced stages than lower stages (***Figure 15 A.***, ***C.*** and ***D.***). Nonetheless, NOP2 did not present statistical differences among different pathological stages (***Figure 15 B.***).

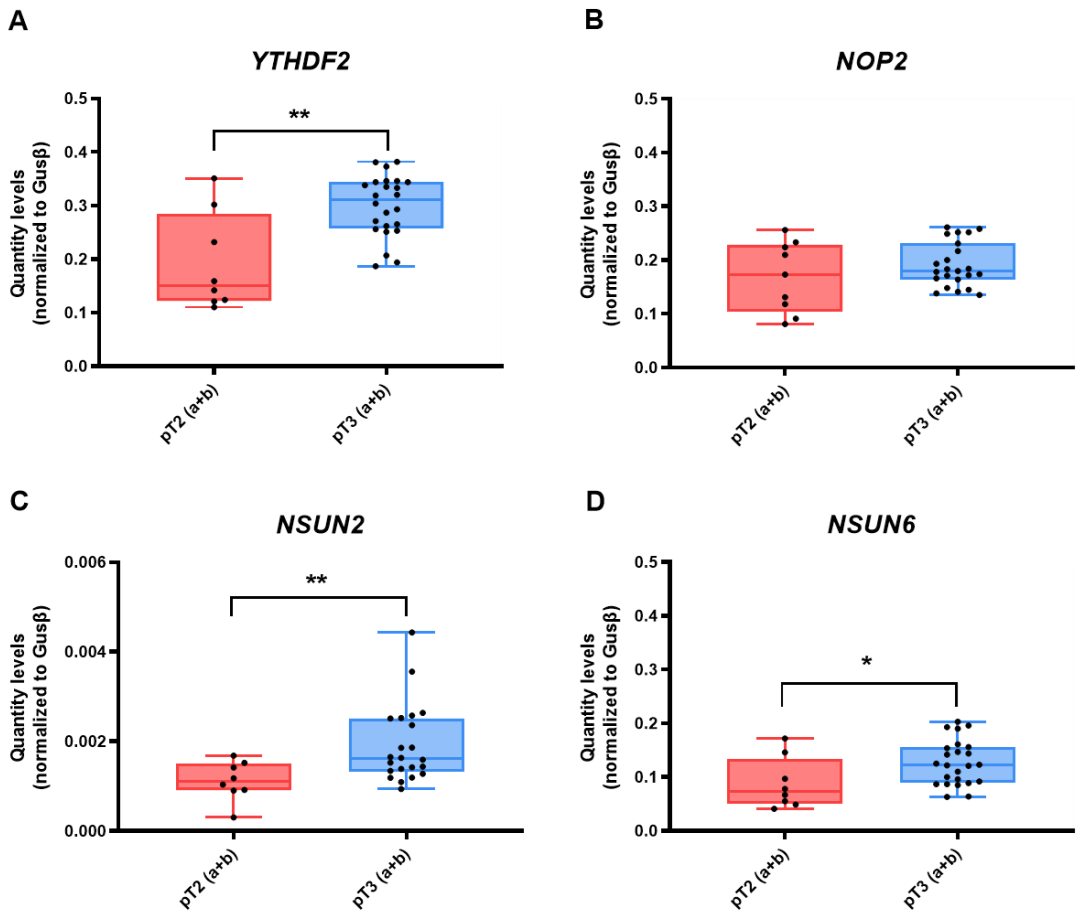

Figure 15. **Transcript levels of *YTHDF2*, *NOP2*, *NSUN2* and *NSUN6* in PCa patients, grouped by tumor stage (pT2 a+b and pT3 a+b).** All transcript levels were normalized to a housekeeping gene (Gusβ). Statistics from Mann-Whitney tests, where **p*<0.05, ***p*<0.01, ****p*<0.001 and *****p*<0.0001. **A.** *YTHDF2* gene levels (pT2 (a+b) n=8; pT3 (a+b) n=24). **B.** *NOP2* gene levels (pT2 (a+b) n=9; pT3 (a+b) n=23). **C.** *NSUN2* gene levels (pT2 (a+b) n=8; pT3 (a+b) n=22). **D.** *NSUN6* gene levels (pT2 (a+b) n=8; pT3 (a+b) n=24).

Evaluation of NSUN2 in PCa patients' samples through IHC

IHC was performed on the matched slides of PCa patients' cohort for the writer NSUN2, along with 10 cases of normal prostate tissue from CP.

NSUN2 was located mainly in the nucleus, but was also present in the cytoplasm. Illustrative images of the IHC assay can be seen below (***Figure 16***).

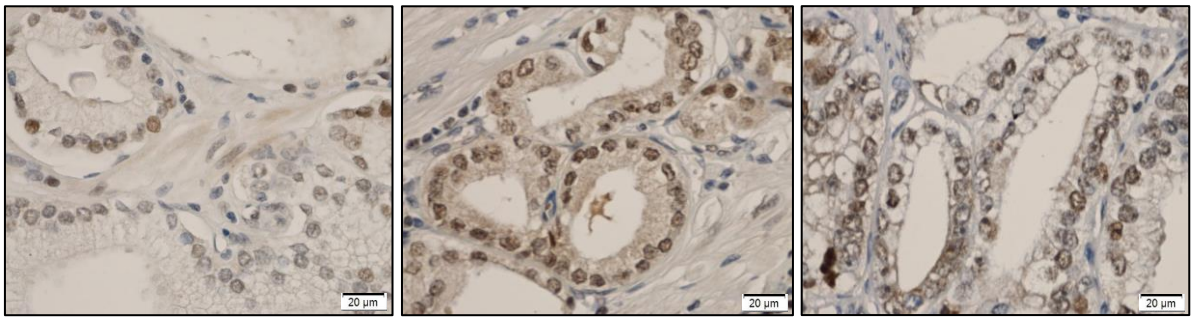

Figure 16. **Illustrative images of immunostaining for NSUN2 protein.** From left to right, can be seen normal prostate tissue (CP), lowest grade PCa (GG1) and highest grade PCa (GG5). Pictures were taken with Olympus BX41 microscope and Olympus U-TV0.63XC digital camera (40x amplification).

In line with transcript levels, the IHC results grouped by GG show that higher NSUN2 immunostaining scores are significantly associated with higher GG, where 14% of these cases showed the highest score (***Figure 17 A.***). Regarding the staining intensity, the differences between normal tissue and PCa GG are even more evident: the lower GG group presented a higher percentage of cases with intensity 2 than normal tissue (53% versus 40%, respectively), while the highest intensity was only found in higher PCa GG (28% of its total cases) (***Figure 17 B.***).

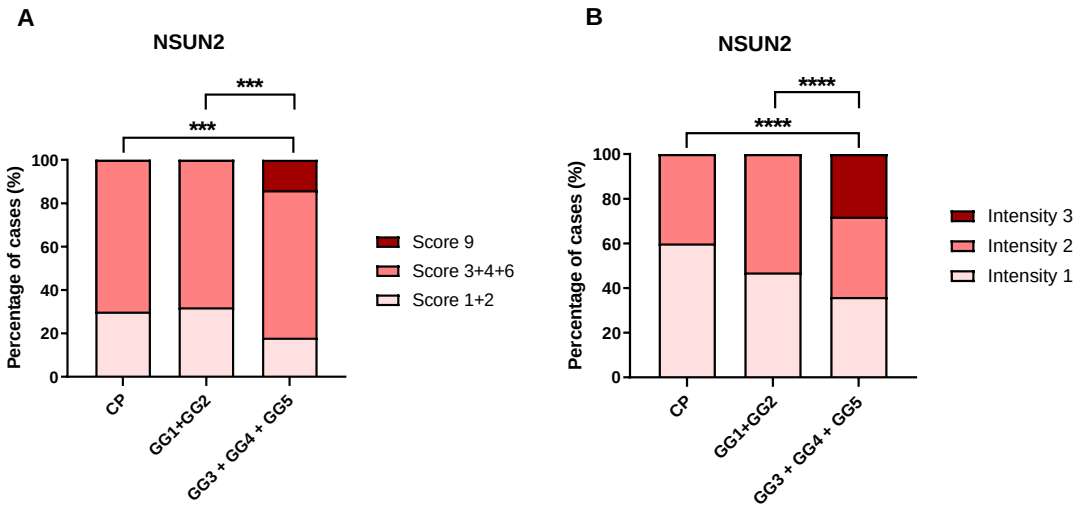

Figure 17. **Characterization of NSUN2 in normal prostate and PCa tissues by IHC, categorized by GG.** Results grouped by CP (normal prostate) (CP n=10), lower GG (1+2) (GG1+GG2 n=19) and higher GG (3+4+5) (GG3+GG4+GG5 n=22). Statistics from Chi-square test, where *p<0.05, **p<0.01, ***p<0.001 and ****p<0.0001. **A.** Immunostaining h-scores (Intensity x Percentage), grouped by low score (1+2), medium score (3+4+6) and high score (9). **B.** Intensity levels, that range from 1 to 3.

Furthermore, when grouped by pathological stage significant differences in immunostaining scores were shown. Higher NSUN2 expression scores were displayed by tumors compared with normal tissue. Moreover, 11% of lower-stage PCa were score as 9, and are representative of a subset of pT2b tumors with aggressive features (***Figure 18 A.***). Additionally, NSUN2 intensity staining increased in higher stage groups, with 9% of pT3 cases presenting intensity higher than 2 (***Figure 18 B.***).

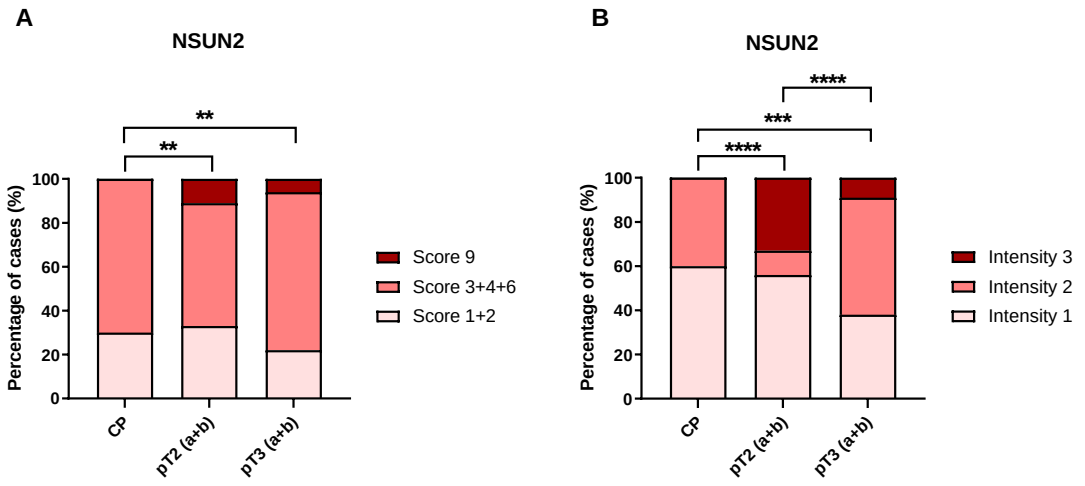

Figure 18. **Characterization of NSUN2 in normal prostate and PCa tissues by IHC, categorized by tumor stage.** Results grouped by CP (normal prostate) (CP n=10), lower tumor stage (pT2 a+b) (pT2 a+b n=9) and higher tumor stage (pT3 a+b) (pT3 a+b n=32). Statistics from Chi-square test, where **p*<0.05, ***p*<0.01, ****p*<0.001 and *****p*<0.0001. **A.** Immunostaining h-scores (Intensity x Percentage), grouped by low score (1+2), medium score (3+4+6) and high score (9). **B.** Intensity levels, that range from 1 to 3.

In vitro evaluation of NSUN2 in PCa cell lines through qPCR and WB

NSUN2 transcript levels were 15-fold higher in C4-2B cell line than in the normal cell line RWPE-1, as it can be seen below (***Figure 19***).

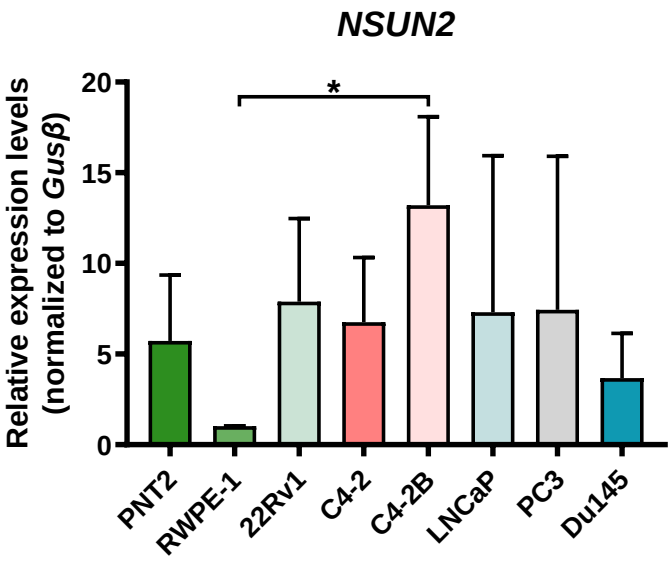

***Figure 19*. Transcript levels of *NSUN2* in prostate cell lines.** All transcript levels were normalized to a housekeeping gene (*Gusβ*). Statistics from Kruskall-Wallis test, where *p<0.05, **p<0.01, ***p<0.001 and ****p<0.0001. Replicate value n=3.

Most PCa cell lines presented higher NSUN2 protein levels than normal/non-malignant cell lines. Importantly, C4-2B cell line NSUN2 levels were the highest, with more than double the protein amount than non-malignant cell lines (***Figure 20***). Hence, C4-2B cell line was chosen for NSUN2 knockdown.

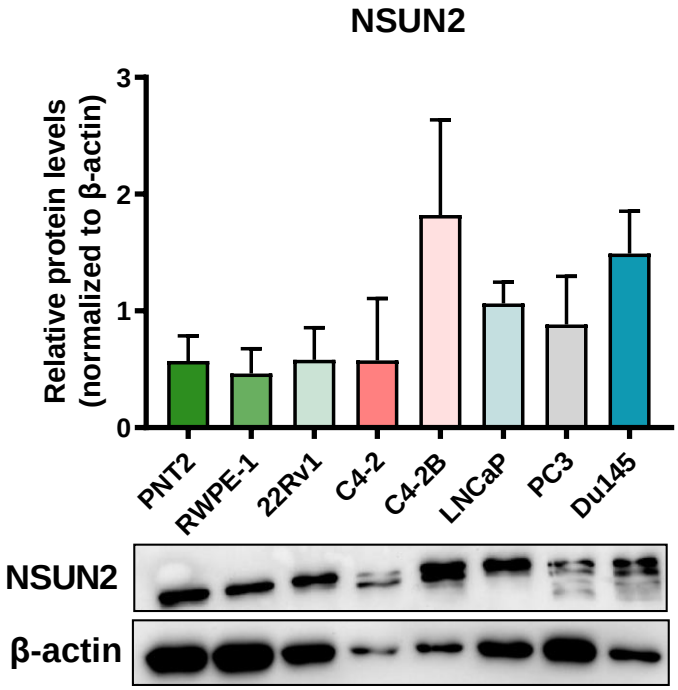

***Figure 20*. Relative protein levels of NSUN2 in prostate cell lines.** All protein levels were normalized to a housekeeping gene (β-Actin). Statistics from Kruskall-Wallis test, where *p<0.05, **p<0.01, ***p<0.001 and ****p<0.0001. Replicate value n=3.

Cell line transduction and establishment

The successful shRNA vectors transduction was attained, as observed in the GFP fluorescent C4-2B cells in culture (***Figure 21***).

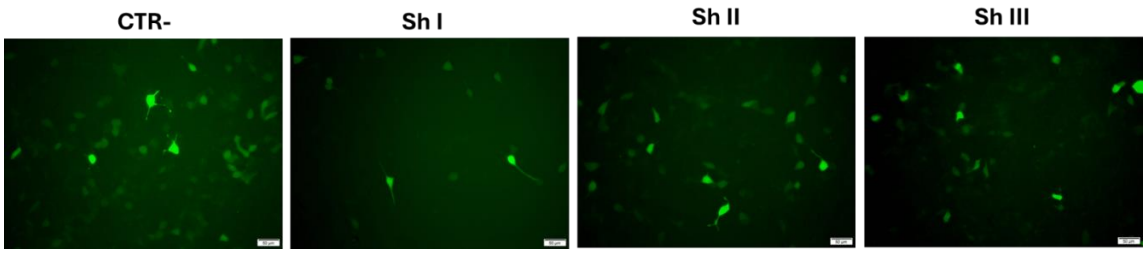

***Figure 21*. Illustrative images of establishment of C4-2B cell line with *NSUN2* gene silencing, with negative control (CTR-) and shRNA vectors (Sh I, II and III).** Photographs taken in Olympus IX51 microscope with Olympus XM10 digital camera (20x amplification).

NSUN2 knockdown was verified by qPCR and Western Blot (***Figure 22***). Although decreased NSUN2 transcript and protein levels were attained with the 3 vectors, cells transduced with Sh I and Sh III vectors presented the highest silencing, 74% and 63%, respectively (***Figure 22 B***). Thus, further evaluations were made with these clones, along with CTR-.

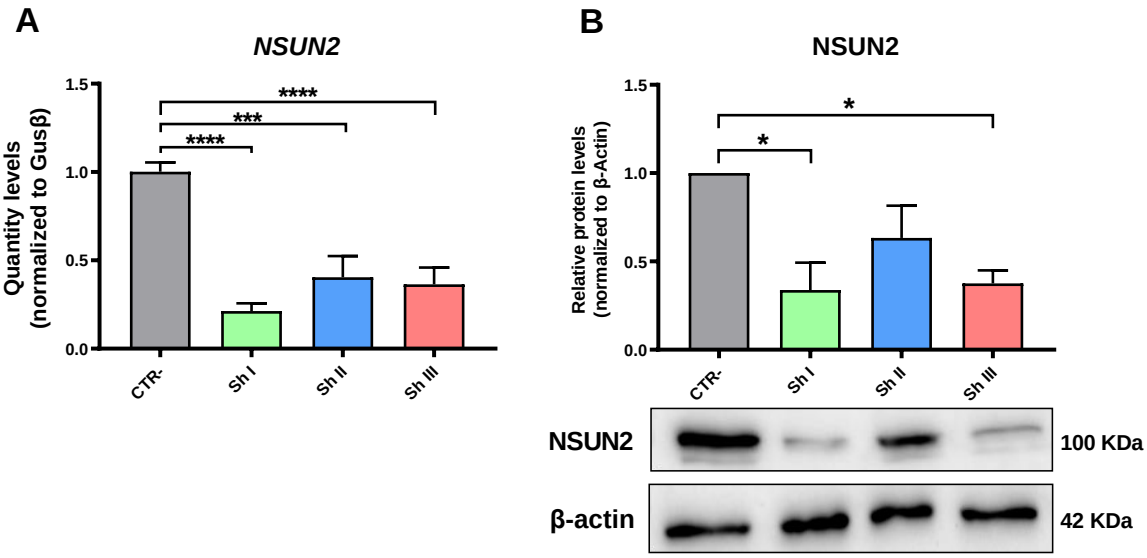

***Figure 22*. Assessment of *NSUN2* silencing of negative control (CTR-) and shRNA vectors (Sh I, II and III).** Statistics from Kruskall-Wallis test, where **p*<0.05, ***p*<0.01, ****p*<0.001 and *****p*<0.0001. **A.** Transcript levels, normalized to *Gusβ* housekeeping gene (n=6). **B.** Relative protein levels, normalized to β-Actin (n=3).

Importantly, C4-2B cells transfected with both Sh I (C4-2B *NSUN2*KD-Sh I) and Sh III (C4-2B *NSUN2*KD-Sh III) presented lower m^5C levels than the control. Moreover, the m^5C mark reduction was more impressive in C4-2B *NSUN2*KD-Sh III cells (***Figure 23***).

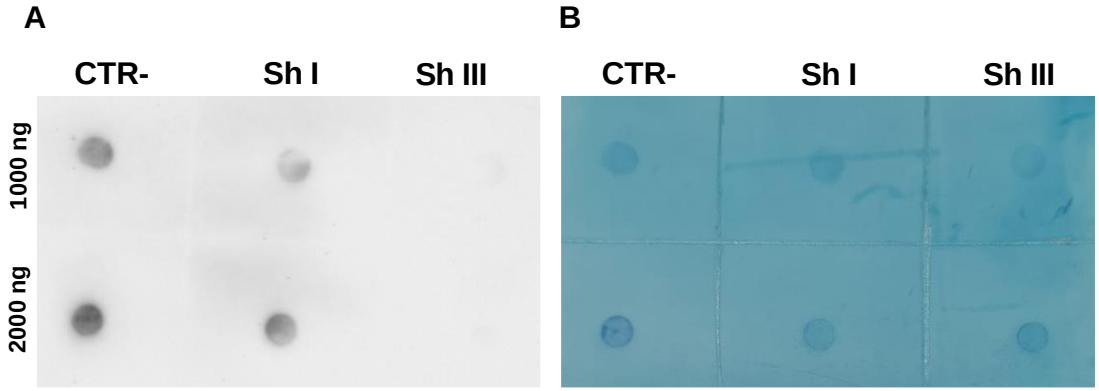

Figure 23. **Assessment of m^5C mark relative levels with Dot Bot of negative control (CTR-) and shRNA vectors (Sh I and III). A.** Relative total levels of m^5C mark attained with chemiluminescence (n=3). **B.** Control dots with methylene blue staining.

Characterization of EMT players after *NSUN2* knockdown in C4-2B cell line

As observed, *NSUN2* knockdown cells presented significantly decreased *CLDN1* and *SNAI1* transcript levels (***Figure 24 B.*** and ***E.***). Contrarily, these cells displayed significantly higher *VIM* transcript levels (***Figure 24 G.***).

Nonetheless, differences were apparent for *TPJ1*, *SNAI2*, and *CDH III* transcript levels between C4-2B *NSUN2*KD-Sh I and C4-2B *NSUN2*KD-Sh III (***Figure 24 A.***, ***D.*** and ***F.***). Moreover, no differences were found for *CDH II* and *CTNNB1* transcript levels upon *NSUN2* knockdown (***Figure 24 C.*** and ***H.***).

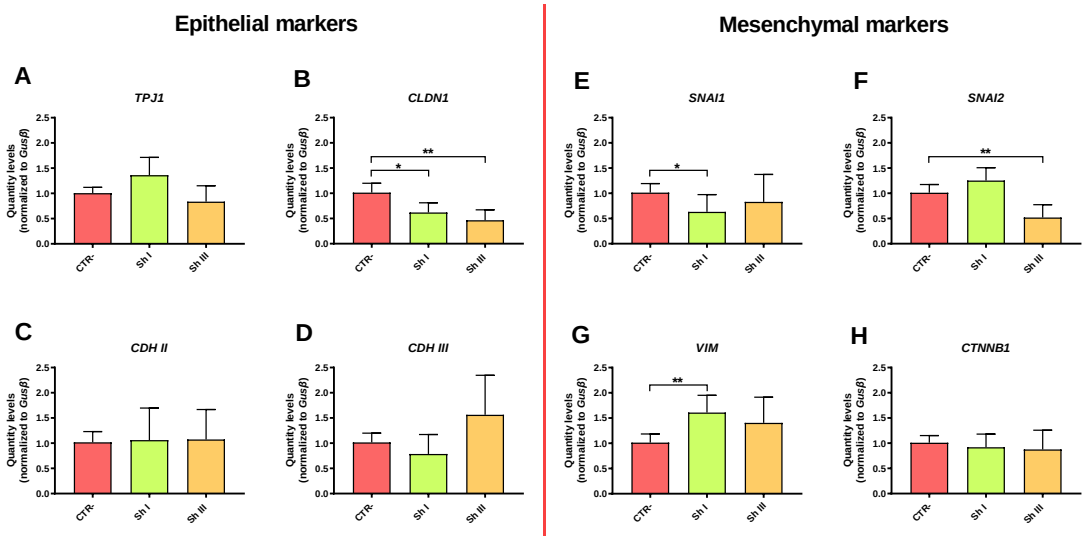

Figure 24. **Transcript levels of EMT-related genes in C4-2B *NSUN2* knockdown cell line.** All levels were normalized to a housekeeping gene (*Gusβ*) (n=3). Statistics from Kruskall-Wallis test, where **p*<0.05, ***p*<0.01, ****p*<0.001 and *****p*<0.0001. **A.** *TPJ1* gene, which codes for ZO-1 protein (n=3). **B.** *CLDN1* gene, which codes for Claudin protein (n=3). **C.** *CDH II* gene, which codes for E-Cadherin

(ECAD) protein (n=3). **D.** *CDH III* gene, which codes for P-Cadherin (PCAD) protein (n=3). **E.** *SNAI1* gene, which codes for SNAIL protein/transcription factor (n=3). **F.** *SNAI2* gene, which codes for SLUG protein/transcription factor (n=3). **G.** *VIM* gene, which codes for Vimentin protein (n=3). **H.** *CTNNB1* gene, which codes for β-Catenin protein (n=3).

At the protein level, all mesenchymal-related proteins (SNAIL, SLUG, Vimentin and β-Catenin) were slightly upregulated in C4-2B NSUN2 knockdown cells, compared with the control (***Figure 25 C.***, ***D.***, ***E.*** and ***F.***), although not reaching statistical significance.

Contrastingly, a tendency of decreased epithelial protein ECAD was found in C4-2B *NSUN2*KD-Sh I, while no alteration was apparent in C4-2B *NSUN2*KD-Sh III (***Figure 25 B.***). Nonetheless, ZO-1, also a protein associated with epithelial phenotype, exhibited an apparent increase in C4-2B *NSUN2*KD-Sh I, but was unaltered in C4-2B *NSUN2*KD-Sh III (***Figure 25 A.***). Parental C4-2B cells did not express Claudins and PCAD, and, therefore, these proteins were not plotted.

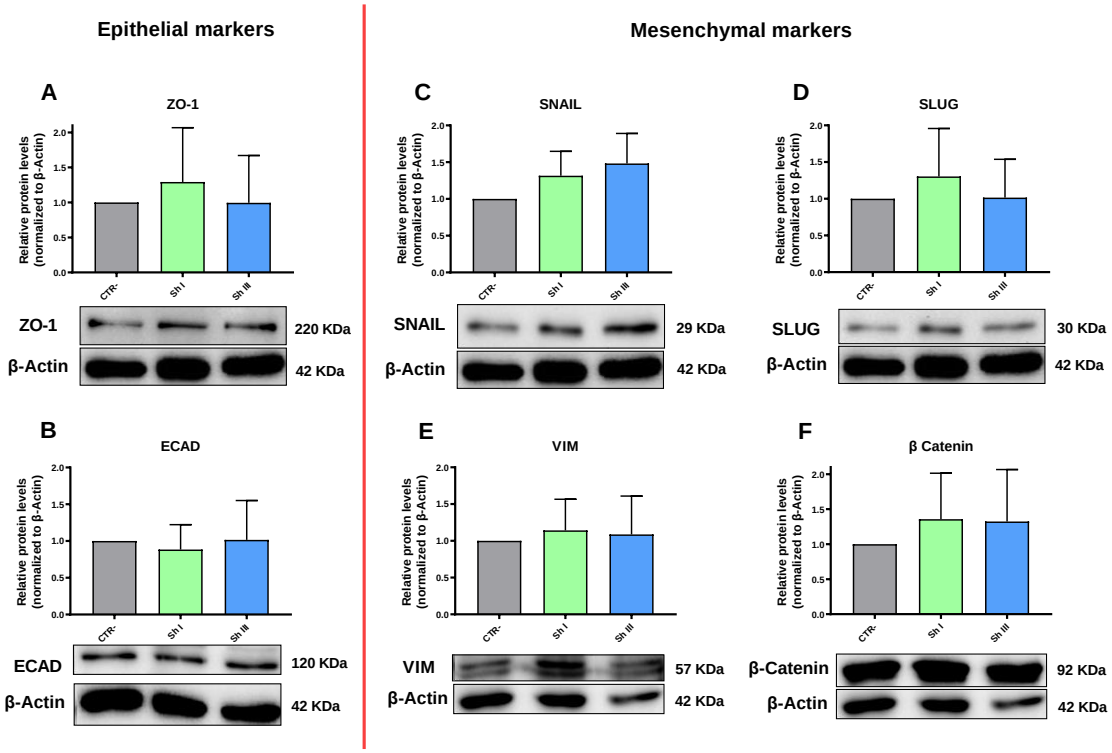

Figure 25. **Relative protein levels of EMT players in negative control (CTR-) and shRNA vectors (Sh I and III).** All levels were normalized to a housekeeping gene (β-Actin) (42 KDa). Statistics from Kruskall-Wallis test, where **p*<0.05, ***p*<0.01, ****p*<0.001 and *****p*<0.0001. **A.** ZO-1 (n=6) **B.** E-Cadherin protein levels (n=3). **C.** SNAIL protein levels (n=4). **D.** SLUG protein levels (n=4). **E.** Vimentin protein levels (n=3). **F.** β-Catenin protein levels (n=3).

DISCUSSION

Discussion

PCa ranks as the second most incident cancer and as the fifth cause of deaths by cancer in males in the world [1]. Most deaths occur at late stages of the disease, where castration resistance and cancer metastasis occur, and treatment options are not effective [70-72]. Besides this, PCa is known for its heterogeneous nature [14]. Consequently, diagnostic and treatment approaches are not adequate for every patient, as they are standardized and lack personalization [73]. Hence, there is a need to better understand the underlying biological mechanisms of PCa progression, and further research is imperative.

Epitranscriptomics is a new research field that investigates the reversible chemical modifications that occur in RNA [43, 44]. Some RNA marks have been recognized as more prevalent in eukaryotes and having a better described link between its functions and cancer, such as m^6A, the first found and most studied epitranscriptomic mark [74-77]. Despite this, other epitranscriptomic marks have been piquing increasing interest to the scientific community [78]. More recently, the m^5C RNA modification was recognized as a very promising epitranscriptomic mark, as it has been linked to a plethora of cancer models, as well as being present in various types of RNA [43, 49, 50]. Nevertheless, much of the functions of RNA modifications in cancer still lack knowledge. Importantly, many m^5C functions remain to be elucidated, especially in the context of PCa.

Herein, this project aims to narrow the understanding between epitranscriptomic regulation and carcinogenesis/progression of PCa. More specifically, we intend to establish a characterization of the m^5C RNA mark in PCa, understanding its significance in the functional and regulatory networks of the disease.

In silico analysis revealed significantly higher mRNA levels of *NOP2*, *NSUN2*, *NSUN6*, as well as increased values of *YTHDF2* in PCa tissues compared to normal prostate tissues. Higher expression in these players had already been implied in other cancer models, such as leukemia, bladder, cervical, lung, and colorectal cancer for YTHDF2 [69], ovarian and colon cancer for NOP2 [79, 80], pancreatic, gastric, and thyroid cancer for NSUN2 [81-83], and cervical, colon and breast cancer for NSUN6 [84-86]. Furthermore, YTHDF2 was associated with tumor suppressor degradation, cancer cell proliferation and PCa progression [87-89]. Thus, these four players were selected for further characterization in patients' samples.

Additionally, transcript levels of the same players were assessed in an independent PCa patient cohort of IPO Porto selected and grouped based on its GG and tumor stage.

Higher *NSUN2* transcript levels were significantly associated with lower PCa differentiation, whereas no significant differences were found for the other players.

However, increased levels of *YTHDF2*, *NSUN2* and *NSUN6* were found in higher tumor stages. Accordingly, NSUN2 was already described to be increased in advanced pathological stages from several other cancers, including head and neck squamous cell carcinoma, uterine corpus endometrial carcinoma, lung squamous cell carcinoma, cervical and esophageal cancer [90]. These results suggest that NSUN2 may act as an unfavorable prognostic marker.

Thus, NSUN2 was selected as the targeted m^5C player for further characterization in patients' tissues by IHC. Predominant nuclear staining of NSUN2 was found, but expression was also found at the cytoplasm. In the same line, other studies also report this protein as being mainly located in the nucleolus [91]. Additionally, recently, NSUN2 was even found in the mitochondria, although its specific functions remain to be elucidated [92].

Moreover, higher NSUN2 immunostaining scores and intensity significantly associated with higher GG, and advanced disease stages. Overall, these results go hand in hand with the previous *in silico* and transcript results.

Additionally, most PCa cell lines displayed higher transcript levels of this m^5C player, in comparison with non-cancerous cell lines, PNT2 and RWPE-1. These results further corroborate that m^5C-related effectors are linked to PCa [93-95]. Furthermore, C4-2B cell line presented the highest and significant fold values of *NSUN2*, with an approximate 15-fold increase. Importantly, similar results were found in protein, where C4-2B cell line presented the biggest NSUN2 protein increase – with an almost 4-fold change, compared to non-malignant cell lines. The metastatic nature of C4-2B cell line, derived from C4-2, that was created from LNCaP [96, 97], may explain these results. Indeed, metastasis-derived cell lines often show more aggressive PCa traits and higher progression-related transcript levels. Regulation mechanisms that were once present in C4-2 cell line may no longer function in C4-2B, as it is a metastasis cell line from C4-2.

Moreover, *in vitro NSUN2* knockdown led to a m^5C significant decrease in the C4-2B cell line, further confirming the pivotal importance of the writer in this RNA methylation mark.

Recently, NSUN2 was determined as a tumorigenesis promoter, with a metastasis-prompting role, by inducing the EMT process in pancreatic cancer [81]. Yet, little to no characterization of NSUN2 role in EMT was achieved in PCa models. Moreover, EMT and its related proteins and transcription factors have been closely associated with cancer progression and metastasis, as it is even considered one of the hallmarks of cancer [22, 28, 29]. Several markers, such as ZO-1, Claudins, SNAIL, SLUG, ECAD, NCAD, PCAD, Vimentin and β-Catenin had previously been described as important to EMT process, even in PCa [98-100].

In our hands, EMT-promoting proteins such as SNAIL, SLUG, VIM and β-Catenin tend to be higher with *NSUN2* knockdown, whereas levels of epithelial-related protein ZO-1 was somewhat decreased. However, no solid conclusions can be taken from these results regarding the function of NSUN2 in the EMT process.

Importantly, NSUN2 has been implicated in other major cell pathways, such as Pi3K/AKT/mTOR in esophageal, lung, kidney and gastric cancers, MAPK/ERK pathway in esophageal and gastric cancers, and RAS pathway in kidney cancer [82, 101-104]. Since all these pathways are known to be implicated in prostate carcinogenesis, one can hypothesize these pathways may be regulated by NSUN2 function.

CONCLUSIONS & FUTURE PERSPECTIVES

Conclusions

These results provide new insights into the role of the main m^5C writer NSUN2 in PCa. As observed, NSUN2 seems to function as an oncogene, since it seems to be associated with malignancy/aggressiveness in the context of prostate carcinogenesis. High levels of this protein were associated with undifferentiated and more advanced tumors. Nonetheless, the function of NSUN2 did not have a major effect on classic EMT-related players.

Whether NSUN2's cancer regulation is model dependent remains unclear, requiring further study in other cancer models. Nevertheless, NSUN2 shows promise as a biomarker for management of PCa.

Future perspectives

In the recent years, epitranscriptomics is revealing itself as a pivotal area for cancer management. The diversity of RNA modifications and their involvement in the most diverse molecular pathways suggest that we are just at the beginning of the RNA epigenetics era in cancer treatment.

The extensive evidence connecting epitranscriptomic dysregulation with cancer strongly indicates that developing inhibitors targeting these RNA pathways could be highly effective. Remarkably, some initial therapies focused on RNA have shown effective results in some types of cancer. Thus, it is expectable that RNA m^5C-related treatments and biomarkers may emerge in a matter of time and research.

Hence, based on our results, several tasks are needed to be performed in a near future:

1. The number of cases evaluated will be increased to strengthen the conclusions drawn from this dissertation.
2. Other prostatic carcinogenesis pathways where NSUN2 has been implicated will be investigated. For this, RNA-seq applied to NSUN2 may help in understanding which cellular pathways might be worth exploring for their impact on PCa development.
3. Other RNA m^5C players will be characterized in the context of PCa, to further elucidate their impact in the m^5C mark and in PCa development and progression.

REFERENCES

References

1. Bray, F., et al., *Global cancer statistics 2022: GLOBOCAN estimates of incidence and mortality worldwide for 36 cancers in 185 countries*. CA Cancer J Clin, 2024.
2. Chen, S., et al., *Estimates and Projections of the Global Economic Cost of 29 Cancers in 204 Countries and Territories From 2020 to 2050*. JAMA Oncol, 2023. **9**(4): p. 465-472.
3. Peppercorn, J., *Financial Toxicity and Societal Costs of Cancer Care: Distinct Problems Require Distinct Solutions*. Oncologist, 2017. **22**(2): p. 123-125.
4. Bergengren, O., et al., *2022 Update on Prostate Cancer Epidemiology and Risk Factors-A Systematic Review*. Eur Urol, 2023. **84**(2): p. 191-206.
5. Arora, K. and C.E. Barbieri, *Molecular Subtypes of Prostate Cancer*. Curr Oncol Rep, 2018. **20**(8): p. 58.
6. Perdana, N.R., et al., *The Risk Factors of Prostate Cancer and Its Prevention: A Literature Review*. Acta Med Indones, 2016. **48**(3): p. 228-238.
7. Ahmadiyeh, N., et al., *8q24 prostate, breast, and colon cancer risk loci show tissue-specific long-range interaction with MYC*. Proc Natl Acad Sci U S A, 2010. **107**(21): p. 9742-6.
8. Gandaglia, G., et al., *Epidemiology and Prevention of Prostate Cancer*. Eur Urol Oncol, 2021. **4**(6): p. 877-892.
9. Andreasson, J. and T. Johansson, *The Cultural History of the Prostate*, in *Prostate Cancer, Sexual Health, and Ageing Masculinities: Exploring the Achilles' Heel of Men*, J. Andreasson and T. Johansson, Editors. 2024, Springer Nature Switzerland: Cham. p. 15-30.
10. Sathianathen, N.J., et al., *Landmarks in prostate cancer*. Nat Rev Urol, 2018. **15**(10): p. 627-642.
11. Epstein, J.I., et al., *The 2014 International Society of Urological Pathology (ISUP) Consensus Conference on Gleason Grading of Prostatic Carcinoma: Definition of Grading Patterns and Proposal for a New Grading System*. Am J Surg Pathol, 2016. **40**(2): p. 244-52.
12. Epstein, J.I., et al., *The 2005 International Society of Urological Pathology (ISUP) Consensus Conference on Gleason Grading of Prostatic Carcinoma*. Am J Surg Pathol, 2005. **29**(9): p. 1228-42.
13. van Leenders, G., et al., *The 2019 International Society of Urological Pathology (ISUP) Consensus Conference on Grading of Prostatic Carcinoma*. Am J Surg Pathol, 2020. **44**(8): p. e87-e99.
14. Haffner, M.C., et al., *Genomic and phenotypic heterogeneity in prostate cancer*. Nat Rev Urol, 2021. **18**(2): p. 79-92.
15. Cornford, P., et al., *EAU-EANM-ESTRO-ESUR-ISUP-SIOG Guidelines on Prostate Cancer-2024 Update. Part I: Screening, Diagnosis, and Local Treatment with Curative Intent*. Eur Urol, 2024.
16. Schaeffer, E.M., et al., *NCCN Guidelines® Insights: Prostate Cancer, Version 3.2024*. J Natl Compr Canc Netw, 2024. **22**(3): p. 140-150.
17. Donovan, M., et al., *The Clinical Usefulness of Prostate Cancer Biomarkers: Current and Future Directions*, in *Cancer Bioinformatics*, K. Ghedira and H. Yosr, Editors. 2022, IntechOpen: Rijeka. p. Ch. 5.

18. Filella, X., et al., *PCA3 in the detection and management of early prostate cancer*. Tumour Biol, 2013. **34**(3): p. 1337-47.
19. Constâncio, V., et al., *Known epigenetic biomarkers for prostate cancer detection and management: exploring the potential of blood-based liquid biopsies*. Expert Rev Mol Diagn, 2019. **19**(5): p. 367-375.
20. Desai, K., J.M. McManus, and N. Sharifi, *Hormonal Therapy for Prostate Cancer*. Endocr Rev, 2021. **42**(3): p. 354-373.
21. Saad, F. and K. Miller, *Treatment options in castration-resistant prostate cancer: current therapies and emerging docetaxel-based regimens*. Urol Oncol, 2014. **32**(2): p. 70-9.
22. Micalizzi, D.S., S.M. Farabaugh, and H.L. Ford, *Epithelial-mesenchymal transition in cancer: parallels between normal development and tumor progression*. J Mammary Gland Biol Neoplasia, 2010. **15**(2): p. 117-34.
23. van Roy, F., *Beyond E-cadherin: roles of other cadherin superfamily members in cancer*. Nat Rev Cancer, 2014. **14**(2): p. 121-34.
24. Lamouille, S., J. Xu, and R. Derynck, *Molecular mechanisms of epithelial-mesenchymal transition*. Nat Rev Mol Cell Biol, 2014. **15**(3): p. 178-96.
25. Meoli, L. and D. Günzel, *The role of claudins in homeostasis*. Nat Rev Nephrol, 2023. **19**(9): p. 587-603.
26. Gonzalez, D.M. and D. Medici, *Signaling mechanisms of the epithelial-mesenchymal transition*. Sci Signal, 2014. **7**(344): p. re8.
27. Ostrowska-Podhorodecka, Z. and C.A. McCulloch, *Vimentin regulates the assembly and function of matrix adhesions*. Wound Repair Regen, 2021. **29**(4): p. 602-612.
28. Hanahan, D., *Hallmarks of Cancer: New Dimensions*. Cancer Discov, 2022. **12**(1): p. 31-46.
29. Mittal, V., *Epithelial Mesenchymal Transition in Tumor Metastasis*. Annu Rev Pathol, 2018. **13**: p. 395-412.
30. Castellón, E.A., S. Indo, and H.R. Contreras, *Cancer Stemness/Epithelial-Mesenchymal Transition Axis Influences Metastasis and Castration Resistance in Prostate Cancer: Potential Therapeutic Target*. Int J Mol Sci, 2022. **23**(23).
31. Grant, C.M. and N. Kyprianou, *Epithelial mesenchymal transition (EMT) in prostate growth and tumor progression*. Transl Androl Urol, 2013. **2**(3): p. 202-211.
32. Parol-Kulczyk, M., et al., *Clinicopathological significance of the EMT-related proteins and their interrelationships in prostate cancer. An immunohistochemical study*. PLoS One, 2021. **16**(6): p. e0253112.
33. Shi, J., et al., *Tumor microenvironment promotes prostate cancer cell dissemination via the Akt/mTOR pathway*. Oncotarget, 2018. **9**(10): p. 9206-9218.
34. Nieto, M.A., et al., *EMT: 2016*. Cell, 2016. **166**(1): p. 21-45.
35. Waddington, C.H., *An Introduction to Modern Genetics*. 2016.
36. Sharma, S., T.K. Kelly, and P.A. Jones, *Epigenetics in cancer*. Carcinogenesis, 2010. **31**(1): p. 27-36.
37. Jerónimo, C. and R. Henrique, *Epigenetic biomarkers in urological tumors: A systematic review*. Cancer Lett, 2014. **342**(2): p. 264-74.

38. Li, Y., *Modern epigenetics methods in biological research*. Methods, 2021. **187**: p. 104-113.
39. Bolton, E.M., et al., *Noncoding RNAs in prostate cancer: the long and the short of it*. Clin Cancer Res, 2014. **20**(1): p. 35-43.
40. Hombach, S. and M. Kretz, *Non-coding RNAs: Classification, Biology and Functioning*. Adv Exp Med Biol, 2016. **937**: p. 3-17.
41. Rönnau, C.G., et al., *Noncoding RNAs as novel biomarkers in prostate cancer*. Biomed Res Int, 2014. **2014**: p. 591703.
42. Esteve-Puig, R., A. Bueno-Costa, and M. Esteller, *Writers, readers and erasers of RNA modifications in cancer*. Cancer Lett, 2020. **474**: p. 127-137.
43. Primac, I., A. Penning, and F. Fuks, *Cancer epitranscriptomics in a nutshell*. Curr Opin Genet Dev, 2022. **75**: p. 101924.
44. Davalos, V., S. Blanco, and M. Esteller, *SnapShot: Messenger RNA Modifications*. Cell, 2018. **174**(2): p. 498-498.e1.
45. Delaunay, S. and M. Frye, *RNA modifications regulating cell fate in cancer*. Nat Cell Biol, 2019. **21**(5): p. 552-559.
46. Barbieri, I. and T. Kouzarides, *Role of RNA modifications in cancer*. Nat Rev Cancer, 2020. **20**(6): p. 303-322.
47. Jonkhout, N., et al., *The RNA modification landscape in human disease*. RNA, 2017. **23**(12): p. 1754-1769.
48. Frye, M., et al., *RNA modifications modulate gene expression during development*. Science, 2018. **361**(6409): p. 1346-1349.
49. Cheng, J.X., et al., *RNA cytosine methylation and methyltransferases mediate chromatin organization and 5-azacytidine response and resistance in leukaemia*. Nat Commun, 2018. **9**(1): p. 1163.
50. Zhang, Q., et al., *The role of RNA m(5)C modification in cancer metastasis*. Int J Biol Sci, 2021. **17**(13): p. 3369-3380.
51. Toden, S., T.J. Zumwalt, and A. Goel, *Non-coding RNAs and potential therapeutic targeting in cancer*. Biochim Biophys Acta Rev Cancer, 2021. **1875**(1): p. 188491.
52. Zhang, T., et al., *Programmable RNA 5-methylcytosine (m5C) modification of cellular RNAs by dCasRx conjugated methyltransferase and demethylase*. Nucleic Acids Research, 2024. **52**(6): p. 2776-2791.
53. Trixl, L. and A. Lusser, *The dynamic RNA modification 5-methylcytosine and its emerging role as an epitranscriptomic mark*. Wiley Interdiscip Rev RNA, 2019. **10**(1): p. e1510.
54. Song, H., et al., *Biological roles of RNA m(5)C modification and its implications in Cancer immunotherapy*. Biomark Res, 2022. **10**(1): p. 15.
55. Zhang, X., et al., *TET (Ten-eleven translocation) family proteins: structure, biological functions and applications*. Signal Transduct Target Ther, 2023. **8**(1): p. 297.
56. Zaccara, S., R.J. Ries, and S.R. Jaffrey, *Reading, writing and erasing mRNA methylation*. Nature Reviews Molecular Cell Biology, 2019. **20**(10): p. 608-624.
57. Wang, D., et al., *METTL3 promotes prostate cancer progression by regulating miR-182 maturation in m6A-dependent manner*. Andrologia, 2022. **54**(7): p. 1581-1591.

58. Liu, T., et al., *The m6A reader YTHDF1 promotes ovarian cancer progression via augmenting EIF3C translation*. Nucleic Acids Res, 2020. **48**(7): p. 3816-3831.
59. Sun, R., et al., *ALKBH5 activates FAK signaling through m6A demethylation in ITGB1 mRNA and enhances tumor-associated lymphangiogenesis and lymph node metastasis in ovarian cancer*. Theranostics, 2023. **13**(2): p. 833-848.
60. Sun, Y., et al., *METTL3 promotes chemoresistance in small cell lung cancer by inducing mitophagy*. J Exp Clin Cancer Res, 2023. **42**(1): p. 65.
61. Xie, J., et al., *M6A-mediated-upregulation of lncRNA BLACAT3 promotes bladder cancer angiogenesis and hematogenous metastasis through YBX3 nuclear shuttling and enhancing NCF2 transcription*. Oncogene, 2023. **42**(40): p. 2956-2970.
62. Xu, Y., et al., *The N6-methyladenosine METTL3 regulates tumorigenesis and glycolysis by mediating m6A methylation of the tumor suppressor LATS1 in breast cancer*. J Exp Clin Cancer Res, 2023. **42**(1): p. 10.
63. Barros-Silva, D., et al., *VIRMA-Dependent N6-Methyladenosine Modifications Regulate the Expression of Long Non-Coding RNAs CCAT1 and CCAT2 in Prostate Cancer*. Cancers (Basel), 2020. **12**(4).
64. Netto, G.J., et al., *The 2022 World Health Organization Classification of Tumors of the Urinary System and Male Genital Organs-Part B: Prostate and Urinary Tract Tumors*. Eur Urol, 2022. **82**(5): p. 469-482.
65. Dai, Q., et al., *Ultrafast bisulfite sequencing detection of 5-methylcytosine in DNA and RNA*. Nat Biotechnol, 2024.
66. Zhu, W., et al., *Positive epigenetic regulation loop between AR and NSUN2 promotes prostate cancer progression*. Clin Transl Med, 2022. **12**(9): p. e1028.
67. Sun, F., et al., *Long noncoding RNA LINC00963 induces NOP2 expression by sponging tumor suppressor miR-542-3p to promote metastasis in prostate cancer*. Aging (Albany NY), 2020. **12**(12): p. 11500-11516.
68. Zhang, Z., et al., *The functions and mechanisms of RNA modification in prostate: Current status and future perspectives*. Front Genet, 2024. **15**: p. 1380746.
69. Liu, R., et al., *Novel insights into roles of N6-methyladenosine reader YTHDF2 in cancer progression*. J Cancer Res Clin Oncol, 2022. **148**(9): p. 2215-2230.
70. Elmehrath, A.O., et al., *Causes of Death Among Patients With Metastatic Prostate Cancer in the US From 2000 to 2016*. JAMA Netw Open, 2021. **4**(8): p. e2119568.
71. Le, T.K., et al., *Castration-Resistant Prostate Cancer: From Uncovered Resistance Mechanisms to Current Treatments*. Cancers (Basel), 2023. **15**(20).
72. Labriola, M.K., et al., *Management of men with metastatic castration-resistant prostate cancer following potent androgen receptor inhibition: a review of novel investigational therapies*. Prostate Cancer Prostatic Dis, 2021. **24**(2): p. 301-309.

73. Shore, N.D., et al., *Addressing Challenges and Controversies in the Management of Prostate Cancer with Multidisciplinary Teams*. Target Oncol, 2022. **17**(6): p. 709-725.
74. Deng, L.J., et al., *m6A modification: recent advances, anticancer targeted drug discovery and beyond*. Mol Cancer, 2022. **21**(1): p. 52.
75. Cao, X., et al., *m(6)A methylation: a process reshaping the tumour immune microenvironment and regulating immune evasion*. Mol Cancer, 2023. **22**(1): p. 42.
76. Liu, Z., et al., *Biological and pharmacological roles of m(6)A modifications in cancer drug resistance*. Mol Cancer, 2022. **21**(1): p. 220.
77. Wang, Y. and G. Jia, *Detection methods of epitranscriptomic mark N6-methyladenosine*. Essays Biochem, 2020. **64**(6): p. 967-979.
78. Nombela, P., B. Miguel-López, and S. Blanco, *The role of m(6)A, m(5)C and Ψ RNA modifications in cancer: Novel therapeutic opportunities*. Mol Cancer, 2021. **20**(1): p. 18.
79. Yang, S., et al., *Function of m(5)C RNA methyltransferase NOP2 in high-grade serous ovarian cancer*. Cancer Biol Ther, 2023. **24**(1): p. 2263921.
80. Bi, J., Y. Huang, and Y. Liu, *Effect of NOP2 knockdown on colon cancer cell proliferation, migration, and invasion*. Transl Cancer Res, 2019. **8**(6): p. 2274-2283.
81. Zhang, G., et al., *NSUN2 stimulates tumor progression via enhancing TIAM2 mRNA stability in pancreatic cancer*. Cell Death Discov, 2023. **9**(1): p. 219.
82. Hu, Y., et al., *NSUN2 modified by SUMO-2/3 promotes gastric cancer progression and regulates mRNA m5C methylation*. Cell Death Dis, 2021. **12**(9): p. 842.
83. Li, P., et al., *The m(5) C methyltransferase NSUN2 promotes codon-dependent oncogenic translation by stabilising tRNA in anaplastic thyroid cancer*. Clin Transl Med, 2023. **13**(11): p. e1466.
84. Yu, M., et al., *NSUN6-mediated 5-methylcytosine modification of NDRG1 mRNA promotes radioresistance in cervical cancer*. Mol Cancer, 2024. **23**(1): p. 139.
85. Cui, Y., P. Lv, and C. Zhang, *NSUN6 mediates 5-methylcytosine modification of METTL3 and promotes colon adenocarcinoma progression*. J Biochem Mol Toxicol, 2024. **38**(6): p. e23749.
86. Huang, Z., et al., *Prognostic Significance and Tumor Immune Microenvironment Heterogenicity of m5C RNA Methylation Regulators in Triple-Negative Breast Cancer*. Front Cell Dev Biol, 2021. **9**: p. 657547.
87. Li, J., et al., *YTHDF2 mediates the mRNA degradation of the tumor suppressors to induce AKT phosphorylation in N6-methyladenosine-dependent way in prostate cancer*. Mol Cancer, 2020. **19**(1): p. 152.
88. Zhao, X., et al., *YTHDF2 protein stabilization by the deubiquitinase OTUB1 promotes prostate cancer cell proliferation via PRSS8 mRNA degradation*. J Biol Chem, 2024. **300**(4): p. 107152.
89. Du, C., et al., *Activation of the KDM5A/miRNA-495/YTHDF2/m6A-MOB3B axis facilitates prostate cancer progression*. J Exp Clin Cancer Res, 2020. **39**(1): p. 223.

90. Zheng, L., et al., *NOP2/Sun RNA methyltransferase 2 is a potential pan-cancer prognostic biomarker and is related to immunity*. PLoS One, 2023. **18**(9): p. e0292212.
91. Khan, M.A., et al., *Mutation in NSUN2, which encodes an RNA methyltransferase, causes autosomal-recessive intellectual disability*. Am J Hum Genet, 2012. **90**(5): p. 856-63.
92. Shinoda, S., et al., *Mammalian NSUN2 introduces 5-methylcytidines into mitochondrial tRNAs*. Nucleic Acids Res, 2019. **47**(16): p. 8734-8745.
93. Xu, Z., et al., *Roles of m5C RNA Modification Patterns in Biochemical Recurrence and Tumor Microenvironment Characterization of Prostate Adenocarcinoma*. Front Immunol, 2022. **13**: p. 869759.
94. Li, M., et al., *5-methylcytosine RNA methyltransferases and their potential roles in cancer*. J Transl Med, 2022. **20**(1): p. 214.
95. Gu, X., et al., *Vital roles of m(5)C RNA modification in cancer and immune cell biology*. Front Immunol, 2023. **14**: p. 1207371.
96. Saranyutanon, S., et al., *Cellular and Molecular Progression of Prostate Cancer: Models for Basic and Preclinical Research*. Cancers (Basel), 2020. **12**(9).
97. Thalmann, G.N., et al., *LNCaP progression model of human prostate cancer: androgen-independence and osseous metastasis*. Prostate, 2000. **44**(2): p. 91-103 Jul 1;44(2).
98. Zhang, Q., et al., *Interleukin-17 promotes prostate cancer via MMP7-induced epithelial-to-mesenchymal transition*. Oncogene, 2017. **36**(5): p. 687-699.
99. Begemann, D., H. Anastos, and N. Kyprianou, *Cell death under epithelial-mesenchymal transition control in prostate cancer therapeutic response*. Int J Urol, 2018. **25**(4): p. 318-326.
100. Odero-Marah, V., et al., *Epithelial-Mesenchymal Transition (EMT) and Prostate Cancer*. Adv Exp Med Biol, 2018. **1095**: p. 101-110.
101. Su, J., et al., *NSUN2-mediated RNA 5-methylcytosine promotes esophageal squamous cell carcinoma progression via LIN28B-dependent GRB2 mRNA stabilization*. Oncogene, 2021. **40**(39): p. 5814-5828.
102. Du, X., et al., *NSUN2 promotes lung adenocarcinoma progression through stabilizing PIK3R2 mRNA in an m(5)C-dependent manner*. Mol Carcinog, 2024. **63**(5): p. 962-976.
103. Song, D., et al., *NSUN2-mediated mRNA m(5)C Modification Regulates the Progression of Hepatocellular Carcinoma*. Genomics Proteomics Bioinformatics, 2023. **21**(4): p. 823-833.
104. Xiang, S., et al., *m(5)C RNA Methylation Primarily Affects the ErbB and PI3K-Akt Signaling Pathways in Gastrointestinal Cancer*. Front Mol Biosci, 2020. **7**: p. 599340.

SUPPLEMENTARY DATA

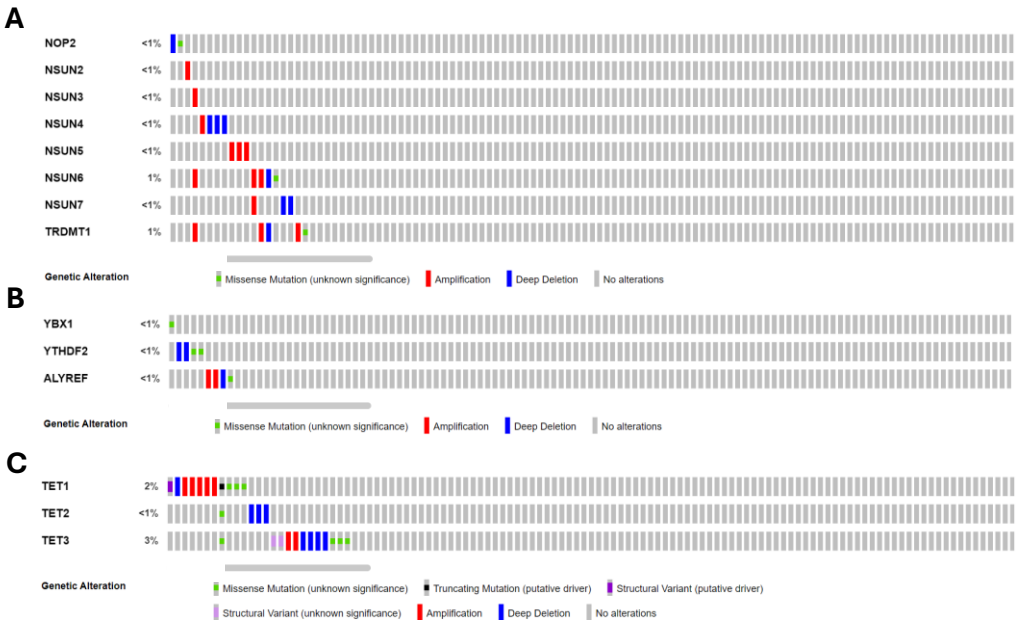

Supplementary Figure 1. **Frequency of genetic alterations in m^{5}C regulators.** From TCGA database. **A.** Writers from NSUN family (NOP2-NSUN7) and TRDMT1. **B.** Readers YBX1, YTHDF2 and ALYREF. **C.** Erasers from TET family (TET1-3).

FACULDADE DE **MEDICINA**